CHAPTER 1

INTRODUCTION

1.1. Background of Study

In 1994, deepwater/ultra-deepwater production sharing contract has been introduced by PETRONAS in order to attract the interest of multinational companies with experience in deepwater exploration, development, and production. As a result, one of the deepwater fields such as Kikeh field project has become the country first deepwater development project in Malaysian history. However, the challenges to develop a deepwater field are much more difficult than the shallow water field especially for the level of Malaysian's expertise. In this case, the formation of hydrate and severe slugging which contribute to the flow assurance problem will be studied.

1.2. Problem Statement

In the deepwater environment such as Kikeh Field, the low temperature and high pressures which encountered by the deepwater riser pipe and flowline can lead to production interruption due to the formation of hydrates and severe slugging. As a result, expensive remedial operations will incur in order to clear the pipelines. PETRONAS has taken the issue very seriously as it could contribute to the low rate of production in the near future. Hence, it is crucial to investigate the condition of the flow patterns in the riser pipe especially in deepwater environment before hydrates and severe slugging mitigation methods can be applied.

1.3. Objectives

The objectives of this project are shown as such:

a) To study the flow characteristic of the oil from the well to the surface which affected by the gas flow rate, oil flow rate and the internal pipeline diameter for Kikeh Field.

b) To investigate the tendency of hydrate formation in the deepwater environment.

1.4. Scope of Study

The study will be focus to the flow characteristic within the riser pipe, which involves:

a) The scope of study is on Kikeh-1 well's PVT information.

b) The type of riser considered is the simple catenary riser (assuming an L-shape riser and horizontal flowline).

c) Anticipated flow patterns from the horizontal flow and vertical flow based on different internal pipeline diameter, oil flow rates and gas flow rates.

d) The formation of hydrates based on the compositional components on Kikeh-1 well's PVT information.

e) The effect of temperature and pressure at different depth, from the sea bed up to surface within the flowline (15 km) and riser (1300 m).

CHAPTER 2

LITERATURE REVIEW

2.1 Flow Assurance in Deepwater Environment (Theory)

‘Flow Assurance’ is a term that encapsulates a number of fluid flow, heat transfer and production chemistry issues that have important implications for the transportation of hydrocarbons from reservoirs to processing facilities.

Deepwater fields present similar flow assurance difficulties to those encountered in the traditional shallow water developments. The ambient temperature in deepwater environments also tends to be lower than the temperature encountered in shallower waters, as well as the surrounding pressure increases due to the increasing of water depth, as in $P_{gauge} = \rho gh$ equation which could promote production interruption due to the formation and deposition of hydrocarbon solids such as hydrates anywhere in the production system. The tendency of hydrate formation will be discussed in the literature review.

Deepwater riser pipes are significantly important for production transportation purposes. The geometric effect of the riser pipes in term of height and internal pipeline diameter could influence severe slugging as well. Various fluid phases flowing from the reservoir rock to the surface and complex reservoir characteristics have to be taken into consideration for hydrate formation. These are flow assurance key risk factors that create significant impact on field development planning, especially, when dealing with marginal deposits having varying fluid characteristics. In addition, the high cost of intervention in deepwater wells and subsea production systems is driving engineers to design inherently reliable and high-availability systems to avoid the need for costly intervention operations [1].

2.2 Hydrate

Hydrates are crystalline solid compound formed from water and guest molecules. Gas hydrates form in untreated multiphase flows when water molecules crystallize around guest molecules at certain pressure and temperature conditions. The most common guest molecules are methane, ethane, propane, isobutane, normal butane, nitrogen, carbon dioxide and hydrogen sulfide, of which methane occurs most abundantly in natural hydrates [2].

Hydrates are known to occur when natural gas and water coexist at elevated pressure and reduced temperature. High pressures and low temperatures are common in deepwater oil and gas fields, which provide ideal conditions for the formation of hydrates. In general, when the multiphase fluid produced at the wellhead flows through the subsea pipelines, it becomes colder, which means most subsea pipelines could experience hydrates at some point in their operating envelope. Moreover, shut-in and startup are also primary times when hydrates form. On shut-in, the line temperature cools to that of the ocean floor so that the system is almost always in the hydrate region if the line is not depressurized [3]. At that condition, multiple hydrate plugs can form.

Figure 2.1 presents a hydrate formation diagram in the pressure-temperature plane. The white region covers pressure and temperature at which hydrates are thermodynamically unstable and is therefore ‘hydrate free’ as indicated. The region labeled ‘hydrate risk’ is where stable hydrates can exist, although in practice they may not be form due to a failure to nucleate and/or slow formation kinetics. In the ‘hydrate zone’ the degree of sub-cooling is sufficient such that hydrates form spontaneously.

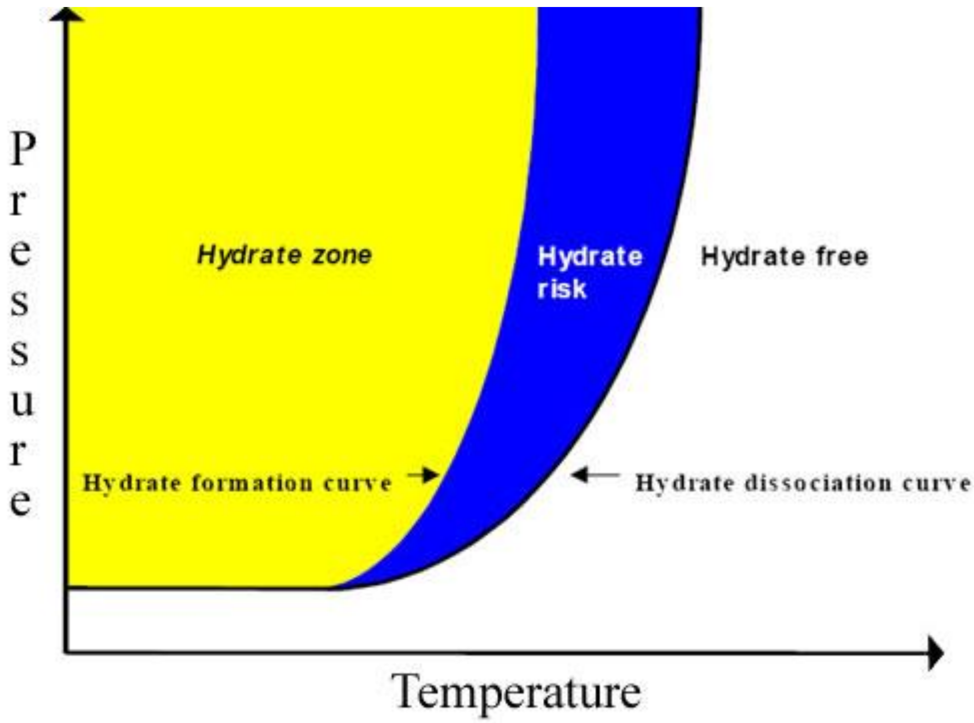

Figure 2.1: Typical hydrate formation diagram [1].

The prediction of hydrate formation in the ‘hydrate risk’ zone is complicated by a number of factors. First, the mechanisms that govern the nucleation of hydrate crystals are essentially random in nature and poorly understood. Moreover, the kinetics of crystal growth are complex being governed by the rate at which water and guest molecules can order themselves into regular lattice structures and the rate at which hydrate formers can be transported through the surrounding phases to the hydrate reaction zone. These mechanisms lead to a time dependency which serves to impede understanding of hydrate formation.

2.2.1 Hydrate Formation Conditions

The formation of hydrate required the following three conditions:

a) The right combination of temperature and pressure. Hydrate formation is favoured by low temperature and high pressure.
b) The hydrate former. Hydrates formers include methane, ethane, and carbon dioxide.
c) A sufficient amount of water.

Other factors that affect hydrate formation include mixing, kinetics, type of physical site, surface for crystal formation, agglomeration and the salinity of the system [4].

2.2.2 Hydrate Structure

Up to now, there are three known structure referred to as structures I, II, and H (abbreviated to sI, sII, and sH). Structure I hydrates contain 46 water molecules per 8 gas molecules giving a hydrate number of 5.75. The water molecules form two small dodecahedral voids and six large tetra decahedral voids. The sizes of the voids are relatively small meaning that the guest molecules are restricted in size to essentially methane and ethane.

Structure II hydrates contain 136 water molecules per 24 gas molecules giving a hydrate number of 5.67. The water molecules form 16 small dodecahedral voids and 8 large hexakaidecahedral voids. The larger voids are able to accommodate molecules including propane, isobutane, cyclopentane, benzene and others.

Structure H hydrates were discovered recently and contain 34 water molecules for every 6 gas molecules giving a hydrate number of 5.67. The structure has three cavity sizes with the largest cavity able to accommodate larger molecules than both sI and sII. sH is unlikely to form unless all of the sII formers are consumed producing sII.

In multiphase oil and gas production pipeline containing hydrocarbon gas, and liquid phases together with a free water phase, hydrates form preferentially at the water-hydrocarbon interface having the highest availability of hydrate forming molecules. Due to smaller cavity sizes of sI, it is well known that this form occurs rarely in oil and gas systems since even small amounts of heavier hydrocarbons (propane and higher) cause sII to be the more stable form. The sI, sII and sH are shown in the Figure 2.2.

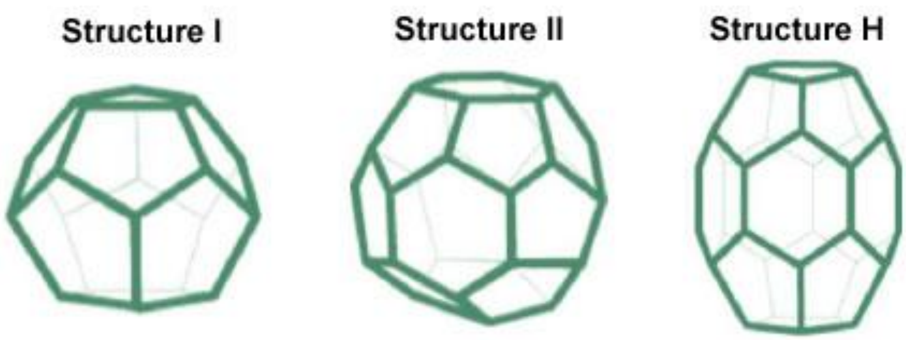

Figure 2.2: Schematic of structure I, II, and H hydrates

2.2.3 K-factor Method for Hydrate Formation Calculation

K-factor method approach can be used to calculate the formation of hydrate which is based of the distribution coefficients (K_i values) for components on a water-free basis [5]. The K-factor is defined as the distribution of the component between hydrate and the gas, $K_i = \frac{y_i}{s_i}$.

2.2.4 Hydrate Problems

Hydrates represent a severe operational problem as the hydrate crystals deposit on the pipe walls and accumulate as large plugs (Figure 2.3), resulting in blocked pipelines, over pressuring and eventually shutdown of production facilities.

Figure 2.3: Hydrate (plug)

The acceleration of these plugs when driven by a pressure gradient can also cause considerable damage to production facilities, and therefore create a severe safety and environmental hazard. The removal of hydrate plugs in subsea production/transmission system poses safety concerns and can be time consuming and costly [6]. For this reason, the hydrate formation in subsea gas transmission pipelines should be prevented effectively and economically to guarantee the pipelines operate normally.

2.2.5 Hydrate Prevention Techniques

Gas hydrate formation can be prevented by several methods such as thermal methods, thermodynamic inhibitors and low dosage hydrate inhibitors. Each method will be explained as such:

a) Thermal methods

Thermal methods use either the conservation or introduction of heat in order to maintain the flowing mixture outside the hydrate formation range. Heat conservation is common practice and is accomplished through insulation (Figure 2.4) or pipe-in-pipe system (Figure 2.5).

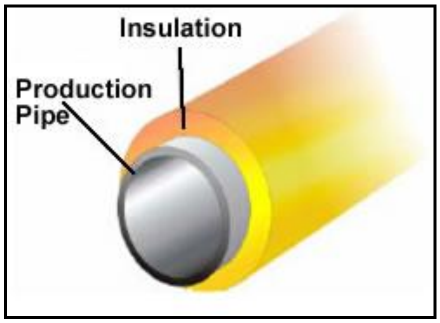

Figure 2.4: Insulation method

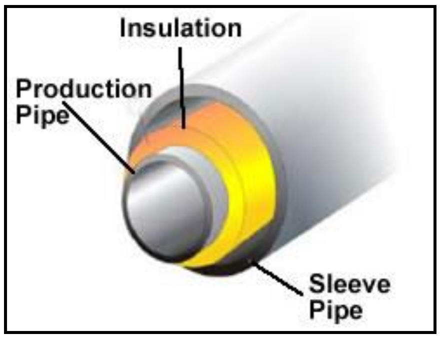

Figure 2.5: Pipe-in-pipe method

Besides, the implementation of electrical heating maybe desirable for long offset systems where available insulation is insufficient to deal with relatively low temperature in deepwater environment or for shut-in condition [7].

b) Thermodynamic inhibitors

Methanol and ethylene glycol are the thermodynamic inhibitors that have the effect of shifting the hydrate formation loci to the left, which causes the hydrate formation point to be displaced to a lower temperature and/or a high pressure.

c) Low dosage hydrate inhibitors (LDHIs)

LDHIs have been actively investigated for the last ten years in both academia and industry [8]. There are two types of LDHIs: the "kinetic hydrate inhibitors" (KHIs), and "anti-agglomerants" (AAs). Kinetic hydrate inhibitors may prevent crystal nucleation or growth during a sufficient delay compared to the residence time in the pipeline. The deeper a system operates in the hydrate region, the shorter the time during which kinetic hydrate inhibitors can delay the hydrate formation. Kinetic inhibitors are relatively insensitive to the hydrocarbon phase and may therefore turn out to be applicable to a wide range of hydrocarbon systems.

Anti-agglomerants are surface active chemicals (i.e. alkyl aromatic sulphonates or alkylphenylethoxylates) do not prevent the formation of hydrate crystal, but keep the particle small and well dispersed so that the fluid viscosity remains low, allowing the hydrates to be transported along with the produced fluids. Anti-agglomerants performance is relatively independent to of time. In addition, anti-agglomerants appear to be effective at more extreme conditions than kinetic hydrate inhibitors, which make these products of interest to operators looking for cost effective hydrate control in deepwater fields [9,10]. These additives are currently applied in the Gulf of Mexico, the North Sea [11] and West Africa.

2.3 Riser (Theory)

Riser pipe is the pipe from the blowout preventer and special fittings on the floating offshore vessel or floating platform to the top of the wellbore. A riser pipe also serves as a guide for the drill stem from the drilling vessel to the wellhead and as conductor for drilling fluid from the well to the vessel.

The riser consists of several sections of pipe and includes special devices to compensate for any movement of the drilling rig caused by the waves. It is also called a marine riser. The vertical portion of a subsea pipeline which including the bottom bend arriving on or departing from a platform. The function of the riser and the type of riser will be discussed as well [12].

2.3.1 Function of Riser

The function of riser in this study is to deliver the oil production from the well to the surface facilities. However, there are several other functions of riser as shown as such:

a) Drilling or production to and from local wells.
b) Hydrocarbon import from remote wells and platform.
c) Hydrocarbon export to shore, to another platform, or to a storage unit.
d) Water or gas injection to increase reservoir pressure for forcing the oil up the well.
e) Hydraulic and electrical lines to control subsea equipment.
f) Workover for well maintenance to keep the oil flowing at a satisfactory rate.

2.3.2 Riser Height and Shape

Riser height will most certainly have an effect on the slugging phenomena as mentioned earlier. The shape of the riser will also play a role. There are different riser shapes: straight upright, S-shape, catenary with a long curvature, and hybrids that is a combination. The sections on riser-stability treated straight upright risers showing that the slugging phenomena were dependent on the riser height in combination with the length of the pipeline upstream of the riser.

The catenary shape will most certainly influence on the stability-limits. Relatively longer risers compared to a conventional riser at the same depth gives increased friction. There will also be different slip between the phases in the bottom of the risers compared to a vertical riser. A third effect is the effect of not having a steep angle of the riser at riser base. These effects must be considered for slugging in steel-catenary risers.

In S-shaped risers the special shape will influence riser-induced slugs. Despite this fact, instabilities in S-risers are classified in the same categorized as for vertical risers: severe slugging, transitional severe slugging, which includes two types, and oscillation flow. The severe slugging has the same characteristics as in vertical risers. So does the transitional severe slugging. The same is the case for oscillating flow that is a rather complex phenomenon in S-shaped risers.

2.3.3 Effect of Riser Diameter

As with oversized well tubing, too large riser give excess gravity pressured drop and instability problems. In addition, riser induced severe slugging may be a result of too large riser, but as described in the basic theory, large riser size can actually prevent severe slugging on the cost of increased pressure drop due to high liquid holdup.

For the offshore oil and gas industry, current design procedure relies on the tenuous extrapolation of correlations based on the results from these small diameter pipes to the larger diameter risers used in practice.

2.3.4 Types of Riser for Different Water Depth

In Malaysia, the water depth of 25 to 200 meters is considered shallow water, whilst 200 meters and more of water depth is considered as deep water. In the shallow water development, conventional riser consisted of steel piping systems are widely used and they are attached to platform jackets. Flexible risers have been used in shallow and moderate water depths as well with floating platforms which they must deal with substantial floating platform or vessel motion. The displacements of these platforms are large relative to water depth and flexible risers have the advantage of being compliant while still fulfilling their function. However, for the deepwater environment, it is not impossible to construct the jacket platforms but it is not feasible due to higher cost of fabrication of steels. Hence, floating systems such as FPSOs (Floating, Production, Storage and Offloading), tension leg platforms (TLPs), spars and semi-submersibles platforms are currently dominate the deepwater production. Until recently, the use of flexible marine risers has been largely unquestioned when floating structures have been employed to develop offshore oil and gas reserves. A major advantage of using a flexible riser was seen to be its compliancy with a vessel's motion. In deeper water, however, the ratio of a vessel's vertical movement to the water depth decreases. This reduces the effective strains applied to a riser due to a vessel's motion and allows alternative riser configurations to be adopted.

Below are the descriptions of type of riser for deep water environment [12]:

a) Rigid Riser

   Rigid risers are vertical lengths of pipe traditionally constructed from steel. As well as steel jacket and concrete gravity structures, rigid risers have been used on compliant towers (Lena, Baldpate), TLPs and spar platforms (Neptune).The ability of rigid risers to accommodate horizontal platform motion increases with water depth. As the length of riser increases, so to the bending flexibility the riser can develops.

b) Flexible Riser

   Flexible risers are constructed from pipe with a layered profile and deform easily in bending while being stiff in response to tension, torsion and internal pressure. Typical configurations of flexible risers include the simple catenary and both the lazy and steep variations of the 'S' and wave catenaries (see Appendix B). Flexible pipe has been used on the deepest field developments to date, and the advent of new profiles in the pressure resisting layers will see the boundaries extended. However, the utilization of flexible pipe in ultra deepwater is restricted by the capabilities of the pipe to withstand high external pressures. The diameters employed at the greater depths are small, as the larger diameter pipes are less capable of withstanding external hydrostatic pressure.

c) Steel Catenary Riser

Steel Catenary Risers (SCRs) consist of pipe (either reeled or of segments welded end to end) hung from a platform down to the sea floor, in a near-catenary shape. A potential advantage of the simple and lazy wave catenary configurations is that the pipe lies parallel to the sea floor and so does not necessarily require installation of a riser base. The steep wave catenary arrangement meets the sea floor nearly perpendicularly and so requires a riser base. For this reason the steep configuration may find application as a production riser, while the other configurations may be well suited to export or import functions. SCRs are fully compliant with vessel motions while only requiring low levels of technology (i.e. a flex or stress joint). The SCR is simple in comparison with the other main riser types - SCRs do not require any heave compensation devices or riser tensioners and can be connected directly to a platform. As such, SCRs are a simple and inexpensive riser for use in water depths greater than 300 meters and are capable of filling a production, import or export function.

d) Hybrid Riser

Hybrid risers (see Appendix B) are a combination of two riser concepts. Basically, the lower portion of the riser consists of either a single rigid pipe or a larger diameter vertical cylinder housing a bundle of smaller production tubes. These rigid sections extend from either a flex or a stress joint at the sea floor and the remaining distance from the top of this rigid section to the platform is spanned by flexible pipe. Hybrid risers exhibit total compliance with a vessel's motions, eliminating the need for heave compensating devices. Significant cost savings may be achieved compared with flexible risers in deepwater, due to the use of rigid, vertical sections of pipe for the lower portion.

2.4 Flow Patterns

Flow patterns for horizontal flow and vertical upward flow are varying to each other in based on the geometry and operating conditions. Hewitt [13] provides an introductory discussion of flow patterns and states that these can themselves be categorized into three types: *dispersed*, *separated* and *intermittent flows*.

Dispersed flows include all flow regimes where one phase is uniformly distributed as roughly spherical elements throughout another continuous phase. Such flows include *bubbly flow* where small gas bubbles are dispersed through a liquid continuous phase.

Separated flows are those where the phases are not intimately mixed. These include *stratified flow* in horizontal pipes where the liquid flows at the base of the pipe with a gas stream flowing above and *annular flow* where the liquid flows around the periphery of the pipe as a thin film with a gas core flowing internally.

Finally, intermittent flows include those where the phases are not distributed uniformly along the pipe, for example *slug flow*. The slug flow pattern is characterized by a chain of bullet-shaped, rising Taylor bubbles. Appendix C presents an illustration of the various flow patterns that exist in vertical and horizontal two-phase flows, At lower gas-liquid ratios, the fluids flow as a bubbly flow with small bubbles of gas distributed throughout the continuous liquid phase (which in oil and gas production is probably itself a water-in-oil dispersion). At higher gas-liquid ratios, the fluids are transported in the annular flow regime. For intermediate gas-oil ratios the slug and churn flow regimes occur and, at high flow rates of both liquid and gas, the *wispy annular flow* regime occurs.

2.4.1 Flow Patterns Calculation

Flow pattern calculations are divided into two which are horizontal flow and vertical flow as such:

a) Horizontal flow

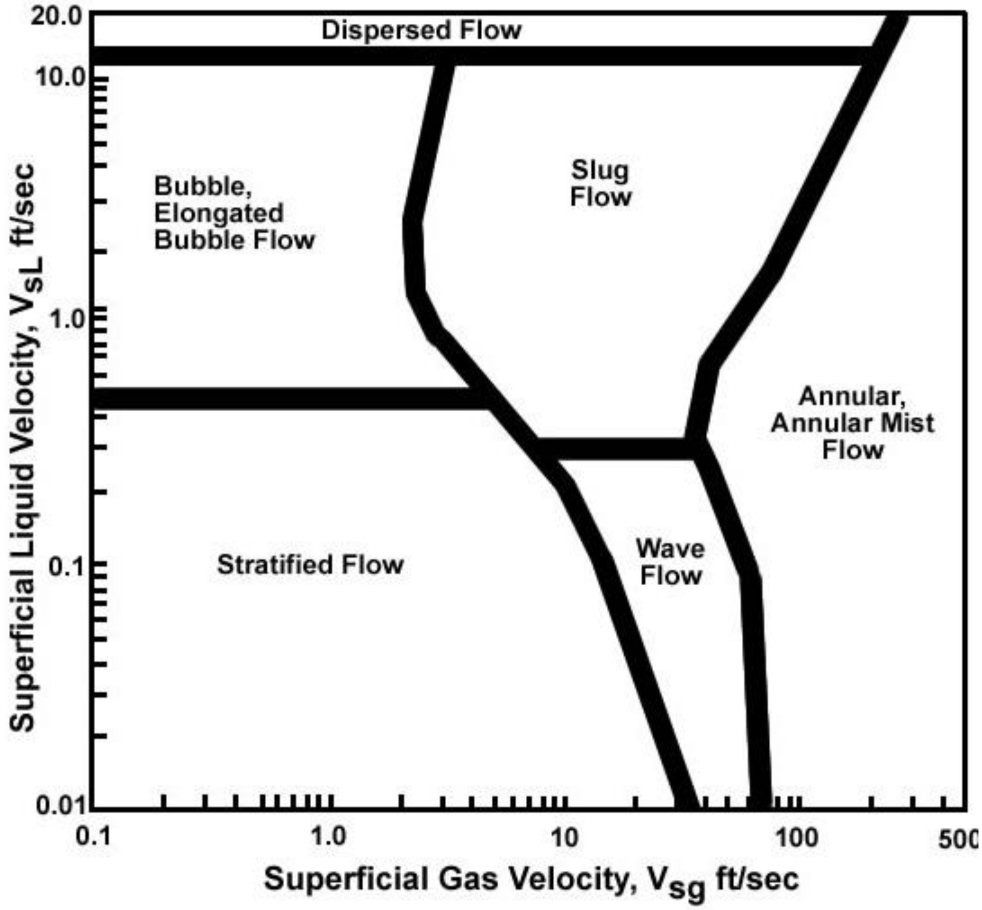

Figure 2.6: Mandhane et al. horizontal flow regime map

Figure 2.6 was the map that developed by Gregory, Aziz and Mandhane [14]. The coordinates of the map are:

$$V_{sL} = Q_L / A \tag{2.1}$$

$$V_{sg} = Q_g / A \tag{2.2}$$

By knowing the xy-coordinates through calculation, the type of flow can be determined from Figure 2.6.

b) Vertical flow

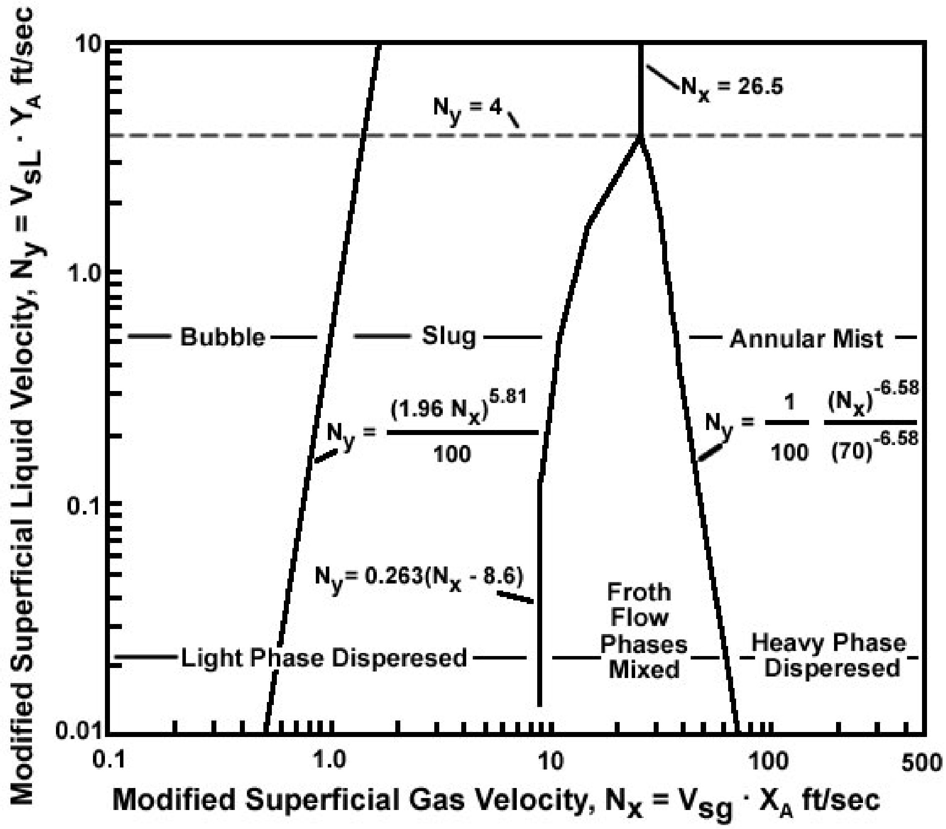

Figure 2.7: Aziz et al. vertical flow regime map

Figure 2.7 shows the vertical flow map which was developed by Aziz[15]. The coordinates for this flow map are the same as for Mandhane map in Figure 2.6 except that the fluid property correction is used. The coordinates used in the Aziz vertical map are:

$$N_x = V_{sg} X_A \tag{2.3}$$

$$N_y = V_{sL} Y_A \tag{2.4}$$

$$Y_A = \left(\frac{\rho_L \sigma_{wa}}{\rho_w \sigma} \right)^{0.25} \tag{2.5}$$

$$X_A = \left(\frac{\rho_g}{\rho_a}\right)^{0.333} Y_A \qquad (2.6)$$

c) Parachor method [5]

It was first reported that vapour-liquid interfacial tension of a pure compound is related to the density difference between the phases as,

$$\sigma = P_\sigma\left(\rho_m^L - \rho_m^V\right) \qquad (2.7)$$

where ρ_m^L and ρ_m^V are the molar density of the liquid and vapour phase, respectively, in gmol/cc and σ is in mN/m or dyne/cm.

The proportionality constant, P_σ, know as *parachor*, has been extensively addressed by Sugden, as a parameter representing the molecular volume of a compound under conditions where the effect of temperature is neutralized. It is considered to have a unique value for each compound independent of pressure and temperature. The parachor values of various pure compounds have been determined from measured interfacial tension data, using Equation 2.7 known as the Macleod-Sudgen equation, reported by several investigators. This equation has been extended to mixture by incorporating various mixing rules. Weinaug and Katz proposed simple molar averaging for the parachor as such:

$$\sigma = \sum P_{\sigma i}\left(x_i \rho_m^L - y_i \rho_m^V\right) \qquad (2.8)$$

where x_i and y_i are the mole fractions of component *i* in the liquid and vapour phase, respectively. $P_{\sigma i}$ is the parachor of component *i*.

2.5 Severe Slugging

A slug is a lump of liquid in a multiphase well stream. Slug flow can pose serious problems to the designer and operator of two-phase flow systems. Large and fluctuating rates of gas and liquid can severely reduce the production and in the worst case shut down or damage topside equipment like separator vessels and compressors. Such instability phenomena such as slugging transitional severe slugging and quasi-stable or oscillation flow can occur in a riser. As a result, prediction of slug characteristics is essential to be considered in the study[1].

Severe slugging is characterized by large pressure fluctuations at the base of the riser and is accompanied by fluctuations in the fluid delivery from the top of the riser. The *severe slugging cycle* is characterized by a noticeable period of constant liquid production followed by a large transient as the liquid column is blown out. Requirement for existence is that the liquid penetrates into the pipeline.

The *transitional severe slugging* is qualitatively similar to the severe slugging but without the constant production period and often an incomplete blow down of the riser. During the transitional slugging the riser base is penetrated by gas prior to the liquid filling the whole riser. These instability phenomena can only exist if the flow is unstable as defined by the Bø criterion.

The *oscillation flow* is a result of oscillatory void fraction in the riser and flowline. This process does resemble severe slugging, but lacks the spontaneous vigorous blowout which is characteristic of severe slugging. The requirement of existence is that the flow is quasi-stable.

As for this study purpose, only severe slugging cycle and the slug flow will be studied more into details.

2.5.1 Process of Severe Slugging Formation in the Riser

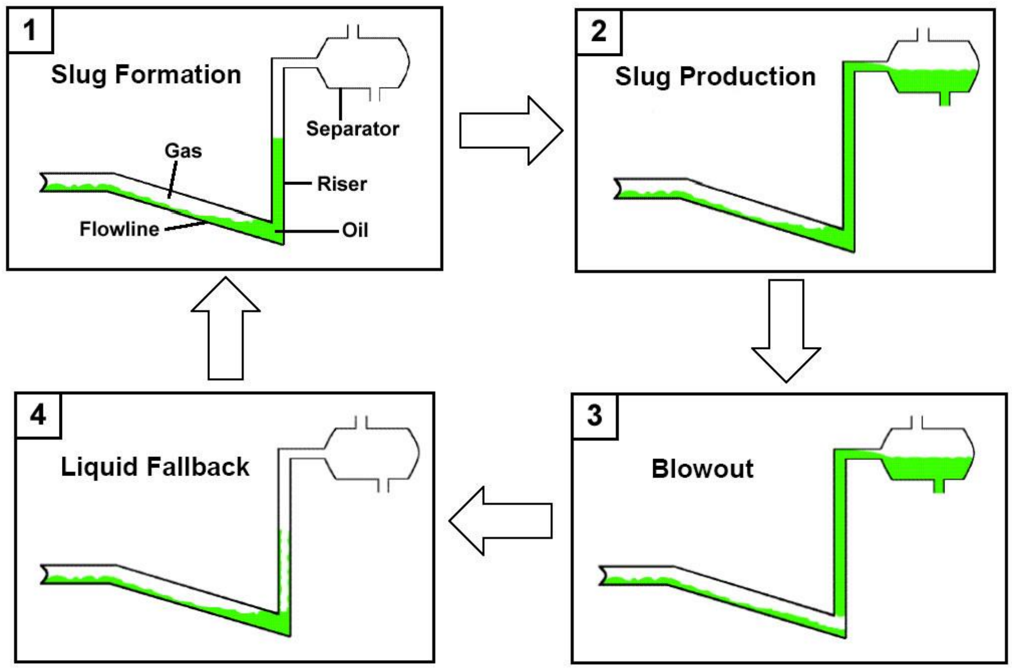

Figure 2.8: Schematic diagram of severe slugging process

As shown in Figure 2.8, it is the cyclic process of the severe slugging formation in the riser. The phenomenon shows the cyclical production of liquid and gas coupled with cyclical pressure fluctuations in the pipeline. The first phase of the cycle is referred to as 'slug formation'. In slug formation the base of the riser has become blocked with liquid preventing free passage of gas. The pressure in the pipeline then increases as more liquid accumulate at the base of the pipeline which increasing the size of the liquid slug. The system remains 'stable' until the pressure has built sufficiently to overcome the gravitational head associated with the liquid slug. The liquid slug is the discharge rapidly up the riser with high pressure, followed immediately by a gas surge as the pipeline blows down. The pressure in the pipeline then returns to a low value, leading to insufficient gas velocities to carry the liquids up the riser, and the whole process is repeated [1].

2.5.2 Problems of Severe Slugging

It is essential to understand what the problems could arise if there is severe slugging. Severe slugging may have undesirable effects on the oil and gas production process. Severe slugging will cause periodic, unstable flow that creates high liquid deliveries, followed by large gas delivery, and finally a no-flow period. This causes overpressure in separators, high level trips and unnecessary flaring of gas.

Besides, the high velocities in the slug tail and the highly fluctuating liquid inventory in the riser induces stresses, reducing operating life and increase the maintenance costs compared to production with even flow. The increased average riser base pressure due to severe slugging reduces the flow from the well.

Furthermore, the increase in backpressure may be sufficient to kill off the well. As opposed to the normal slug, these severe slugs are typically generated at the bottom of a riser [16] or at low elbows [17].

2.5.3 Severe Slugging Prevention Techniques (Theory)

Severe slugging will cause the unpredicted type of flow and it occurred at higher deliveries. Besides there will be a zero flow for a period of time in to the separator even though the gas and liquid are flowing in the flowline [18]. Such situation requires the severe slugging elimination techniques which shown as such:

a) Increase backpressure

Even though the back-pressured imposed in the flowline could eliminate the severe slugging, this option is not viable to be adopted because it will cause the reduction in production capacity.

b) Gas lifting

It is one of the most used methods for the current application. For deepwaters, increased frictional pressure loss and Joule-Thompson cooling are potential problems resulting from high injection gas flow rates. However, the gas lifting must be controlled in order to prevent the severe slugging to occur in the oil pipeline.

c) Choking

Although this is a proven technique to reduce or eliminate severe slugging, careful choking is needed to have the least back-pressure increase for not to experience production reduction. The gas will be choked first in order to accumulate the oil before the choke valve for oil production later (Figure 2.9).

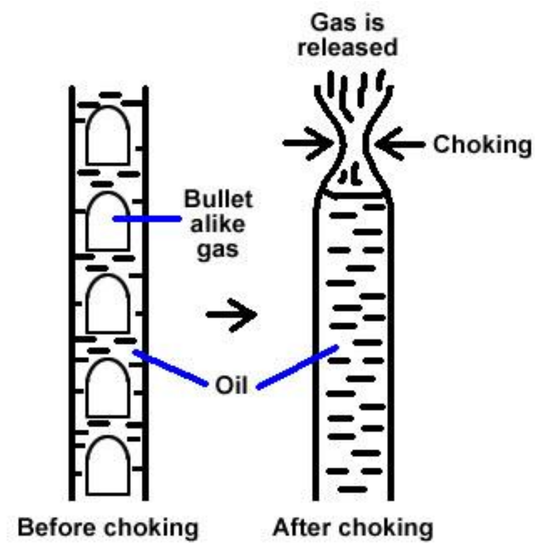

Figure 2.9: Choking at riser top

d) Gas-lift and Choking Combination

Although it is suggested to be a viable method by academia, no field application was reported for current pipeline-riser systems. It might alleviate some of the cooling and excessive frictional pressure loss problems by requiring less injection gas. It will require injection gas and the necessary gas lift installation.

e) Riser Base Pressure Control with a Surface Control

This technique was successfully applied in Totals Dunbar 16” pipeline-riser system. In principle, this technique is very similar to choking. The field data indicated significant overall system pressure increase. It may pose potential production reduction problems for deepwater productions.

f) Subsea Separation

This is a viable solution that does not impose back pressure on the system. But it requires two separate flowlines and a liquid pump to pump the liquids to the surface.

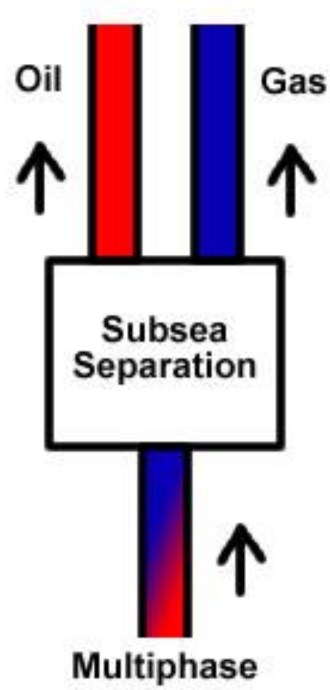

Figure 2.10: Subsea Separation

CHAPTER 3

METHODOLOGY

3.1 The Flow Chart of the Horizontal Flow and Vertical Flow Calculation.

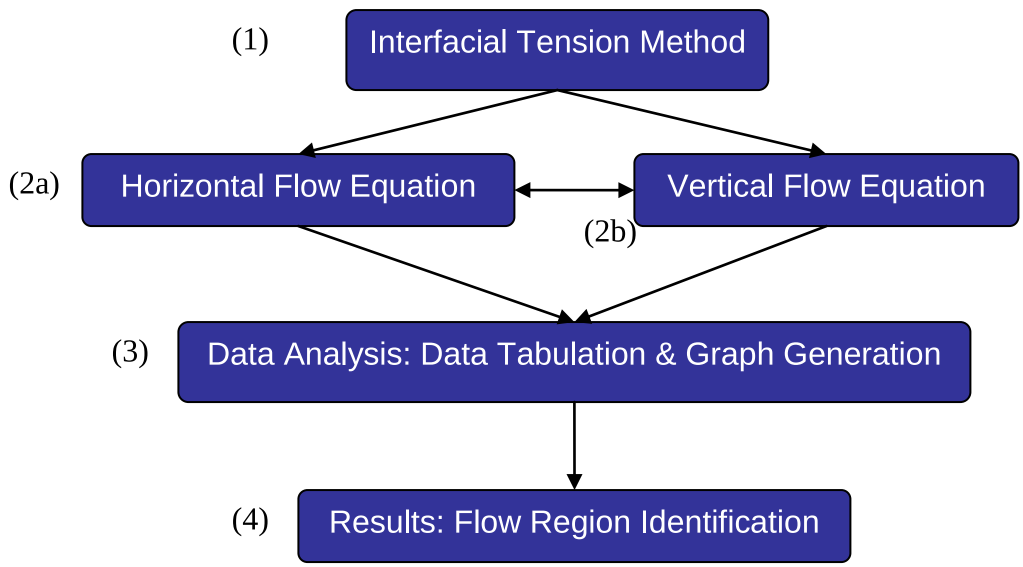

Figure 3.1: Steps of identifying flow patterns

a) Step (1) in Figure 3.1 is to calculate the interfacial tension. Details are in Appendix D.

b) Step (2a) and (2b) is to calculate the horizontal flow by using the Aziz et al. equation and vertical flow by using Mandhane's equation respectively. More details are in Appendix E.

c) Step (3) is to determine and analyse the flow patterns by plotting the values from the horizontal flow equation and vertical flow equation on the graph and compared with Mandhane Horizontal Flow Regime Map and Aziz et a. Vertical Flow Regime Map.

d) Step (4) is the result of the findings which will be reported in Chapter 4.

3.2 The Flow Chart of Generating Hydrate Phase Envelope using PIPESIM

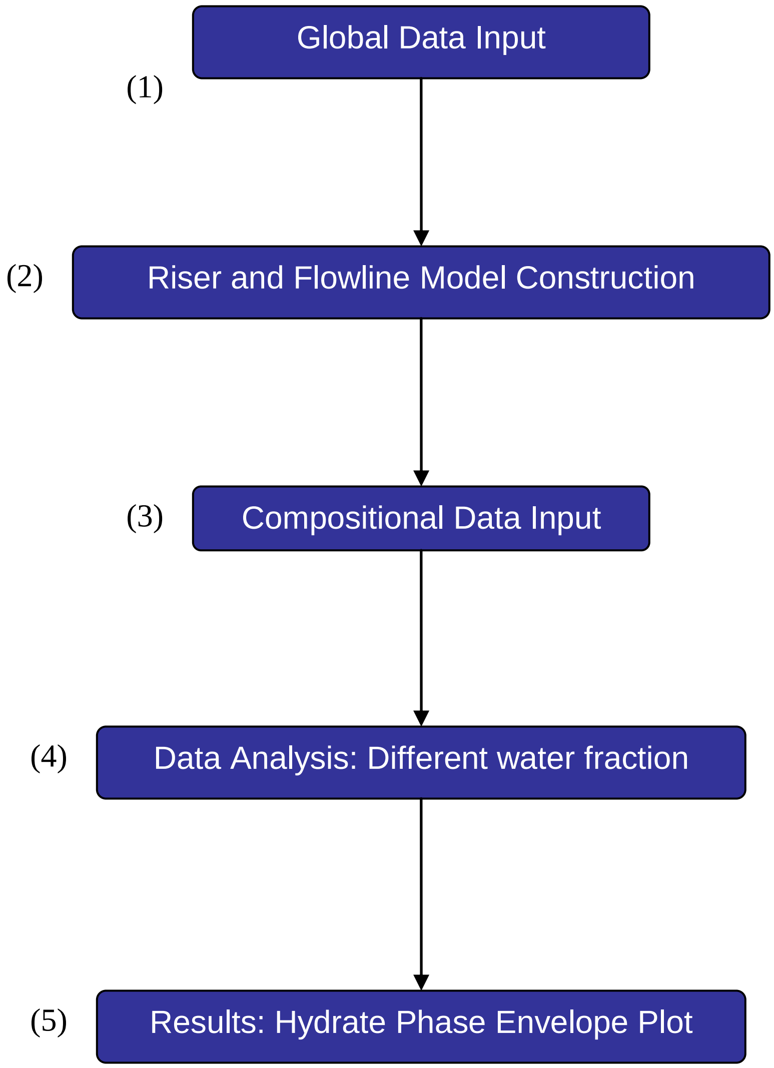

Figure 3.2: Steps of generating hydrate phase envelope using PIPESIM

a) Step (1) in Figure 3.2 is to input the fluid model type, operation type and flow correlations. The chosen fluid type model is Black Oil Model; the chosen operation type is System Analysis; and the chosen flow correlations is Govier, Aziz, Fogarassi for Vertical flow correlation whilst Beggs & Brill Revised for horizontal flow correlation.

b) Step (2) is to construct the flowline model and riser model with specified parameter; Input temperature is 205.5 ˚F; input pressure is 4595 psig; flowline’s length is 15,000 m; and the riser’s height is 1,300 m.

c) Step (3) is to input the values of hydrocarbon component in mole from the PVT test result. These values can be found in Appendix D.

d) Step (4) is to vary the water fraction from 0% bbl/bbl - 100% bbl/bbl. It is to analyse when do the sI hydrate structure, sII hydrate structure and ice will be formed. Besides it is also to analyse the expansion of the hydrate risk region due to the increased water fraction.

e) Step (5) is the result of the findings which will be reported in Chapter 4.

CHAPTER 4

RESULTS AND DISCUSSIONS

4.1 Flow Patterns in Horizontal Flow and Vertical Flow

The horizontal flow occurs in the flowline whilst the vertical flow occurs in the vertical riser pipe. Various internal pipeline diameters (8", 10", 12", 14", and 16" internal diameter) are used in the calculation is to study the type of flow which will be produced at a fixed oil flow rates. Besides, 5 different oil flow rates (9,000 bpd, 11,000 bpd, 13,000 bpd, 15,000 bpd, and 17,000 bpd) are used as the fixed variables. The current production in one riser is estimated to produce at 13,000 bpd. However, for some reasons due to unpredicted reservoir behavior, the 13,000 bpd might be reduced due to pressure depletion or either increased due to sudden water or natural drive mechanism. Therefore, 9,000 bpd, 11,000 bpd, 15,000 bpd, and 17,000 bpd are the extra variables which are used to vary the production flow rates.

Figure 4.1a – 4.1e shows the horizontal flow for 8", 10", 12", 14", and 16" internal pipeline diameters at different oil flow rates, ranging from 9,000bpd to 17,000 bpd. Meanwhile, Figure 4.1f – 4.1j shows the vertical flow for 8", 10", 12", 14", and 16" internal pipeline diameters at different oil flow rates, ranging from 9,000 bpd to 17,000 bpd. Each figure will explain the region of types of flow which will happen in the pipeline at fixed oil flow rate.

4.1.1 Flow Patterns for Horizontal Flow

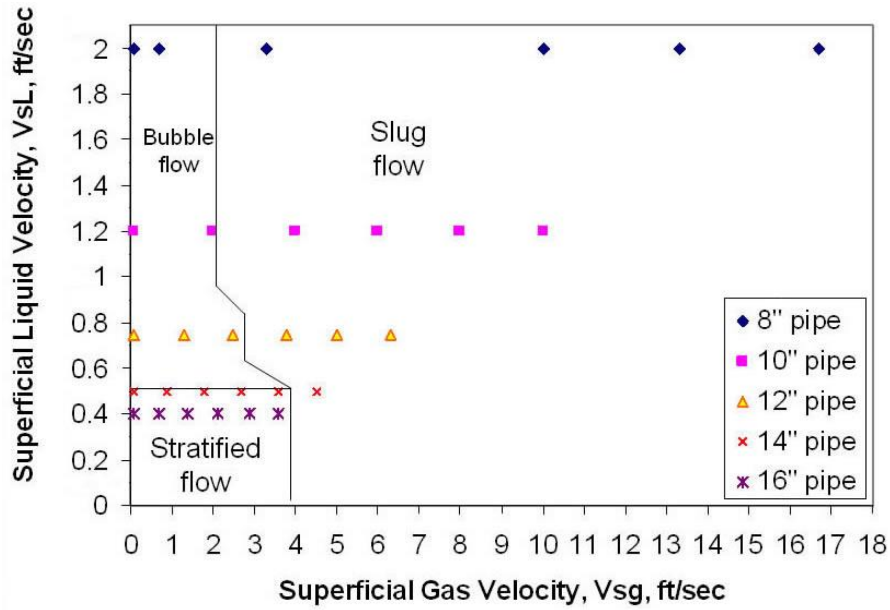

Figure 4.1a: Horizontal flow for different internal pipeline diameters at 9,000 bpd

Figure 4.1a shows that 8”to 14” pipeline will experience slug flow at about Vsg of 4 ft/s and above. Below Vsg of 4 ft/s, 8” to 12” pipeline experiences the bubble flow, but 14” and 16” pipeline experiences stratified flow because they are below VsL of 0.5 ft/s.

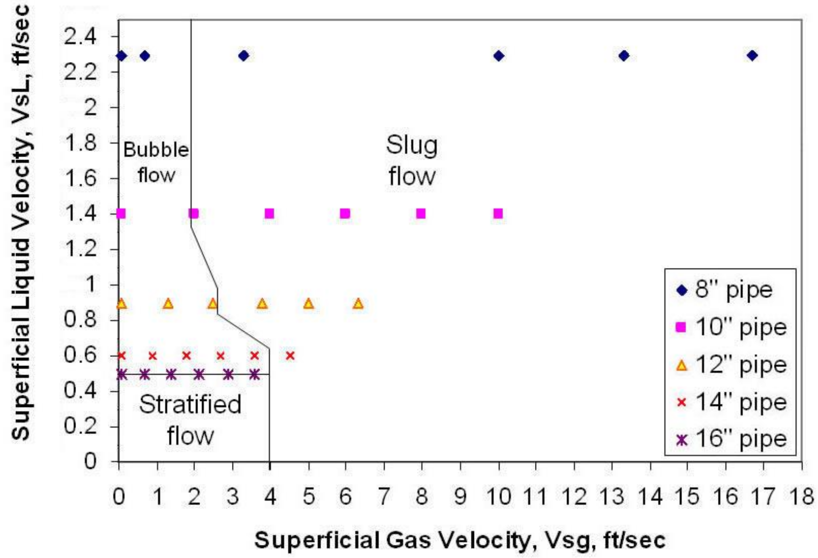

Figure 4.1b: Horizontal flow for different internal pipeline diameters at 11,000bpd

Figure 4.1b shows that when the oil flow rate increased by 2,000 bpd, none any pipeline experiences stratified flow. The result in Figure 4.1b is almost the same with Figure 4.1a.

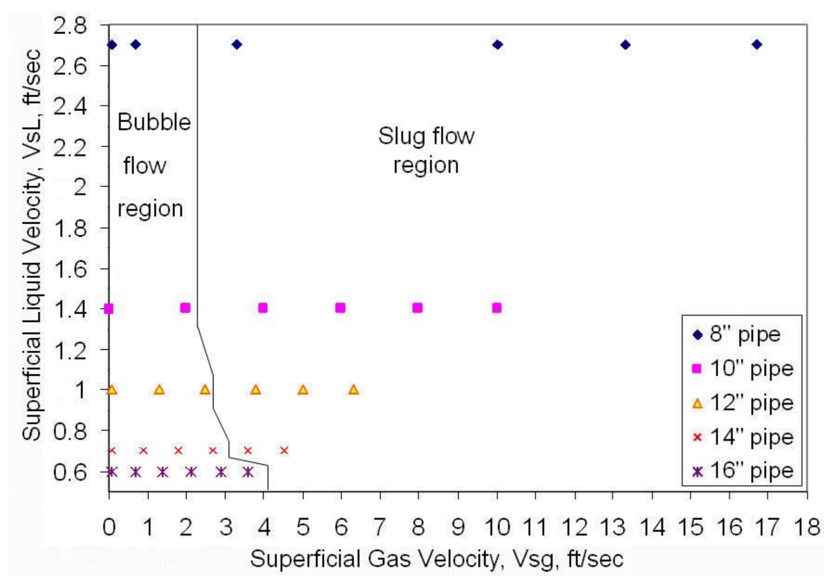

Figure 4.1c: Horizontal flow for different internal pipeline diameters at 13,000 bpd

Figure 4.1c clearly shows that 14" pipeline at Vsg of 3 ft/s experiences slug flow. 16" pipeline still experiences bubble flow at this point.

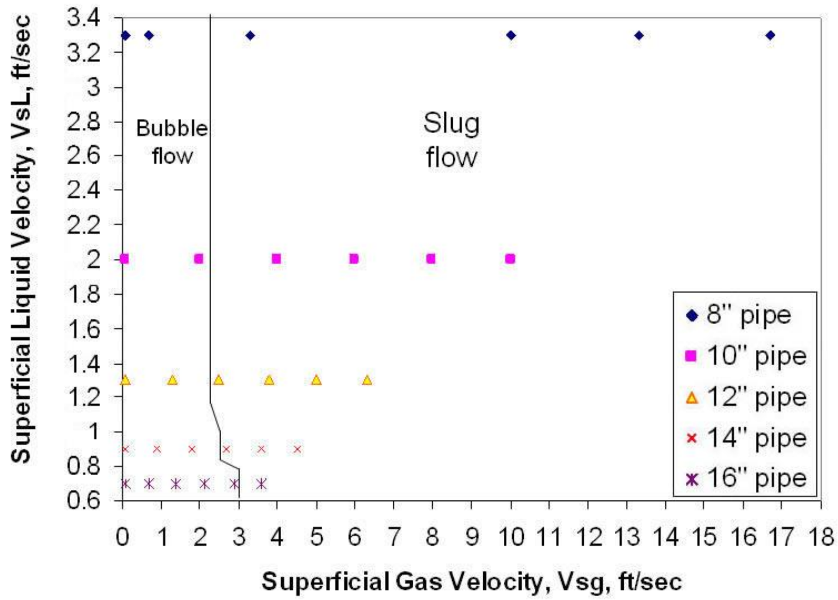

Figure 4.1d: Horizontal flow for different internal pipeline diameters at 15,000 bpd

At 15,000 bpd, 16” pipeline at 3ft/s of Vsg has entered the slug flow region. 8”- 14” pipeline experiences slug flow at about 2.5 ft/s. Besides, the VsL values has no longer influence the type of flow.

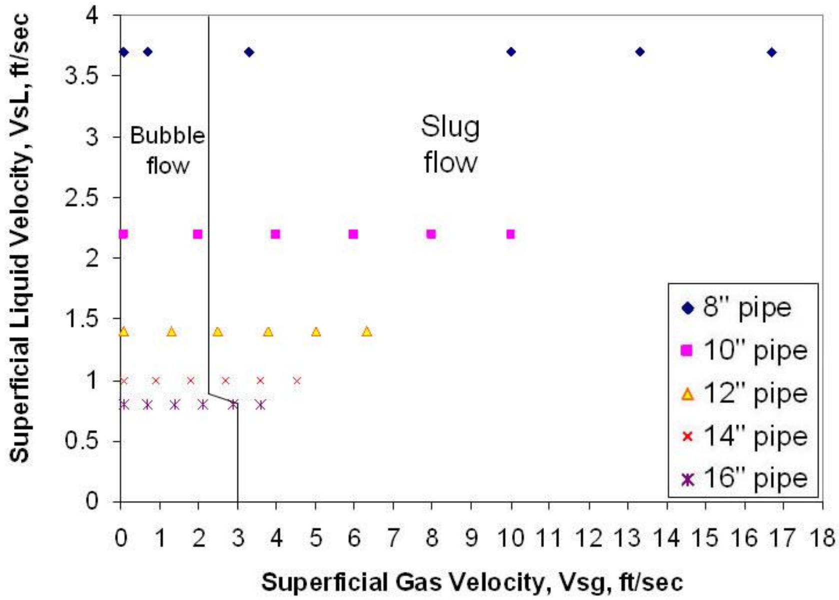

Figure 4.1e: Horizontal flow for different internal pipeline diameters at 17,000bpd

Figure 4.1e show not much difference compare to Figure 4.1d except the 8” to 14” pipeline experiences slug flow at about 2.2 ft/s.

Based on Figure 4.1a to Figure 4.1e, those can be summarized that when the oil flowrate is increased from 9,000 bpd to 17,000 bpd, the slug flow slowly dominating the bubble flow at as the Vsg is lowered. This shows that, the presence of gas in the oil production contribute the slug flow formation. The values in Figure 4.1a to Figure 4.1e which were used to plot those graph can be obtained from Appendix F.

4.1.2 <u>Flow Patterns for Vertical Flow</u>

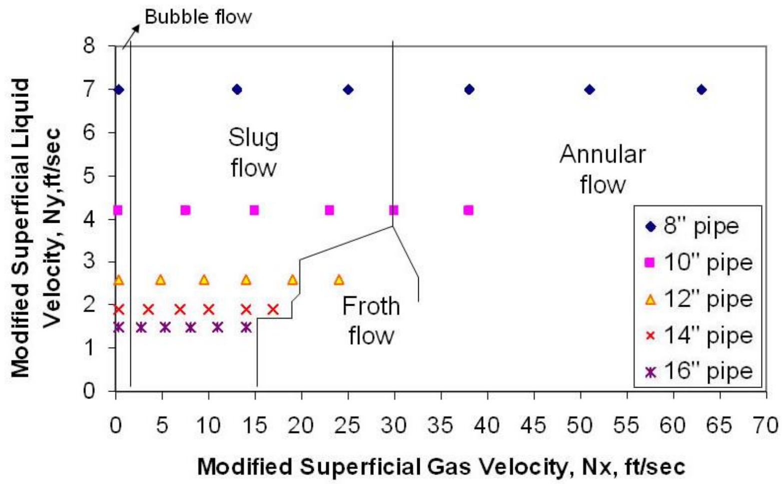

Figure 4.1f: Vertical flow for different internal pipeline diameters at 9,000 bpd

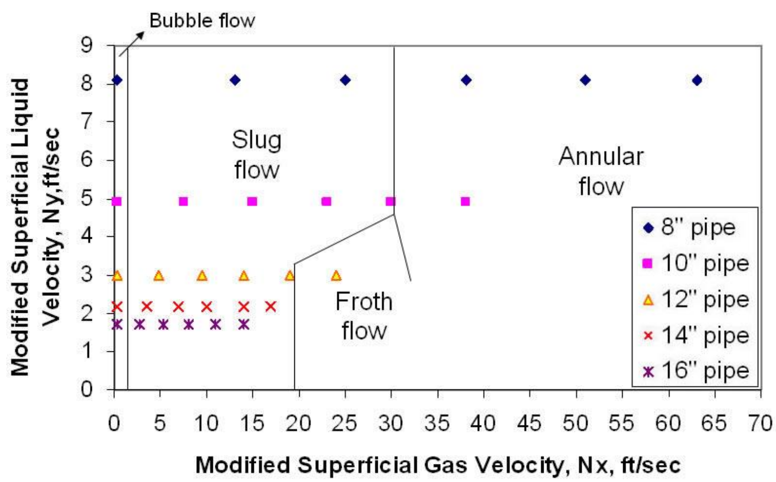

Figure 4.1g: Vertical flow for different internal pipeline diameters at 11,000 bpd

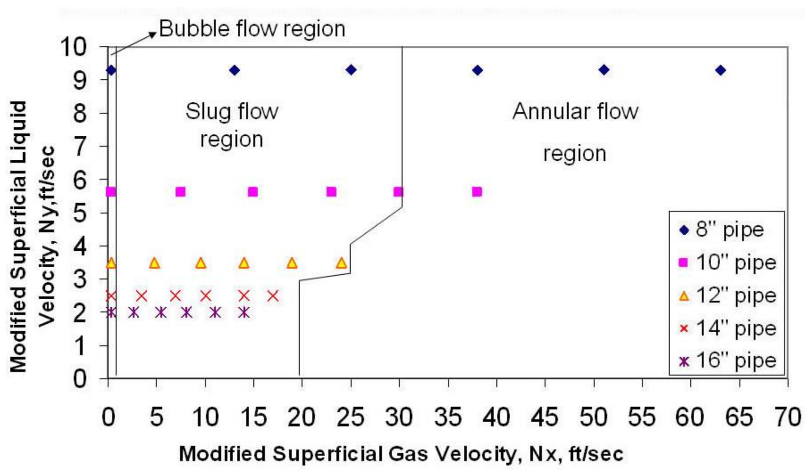

Figure 4.1h: Vertical flow for different internal pipeline diameters at 13,000 bpd

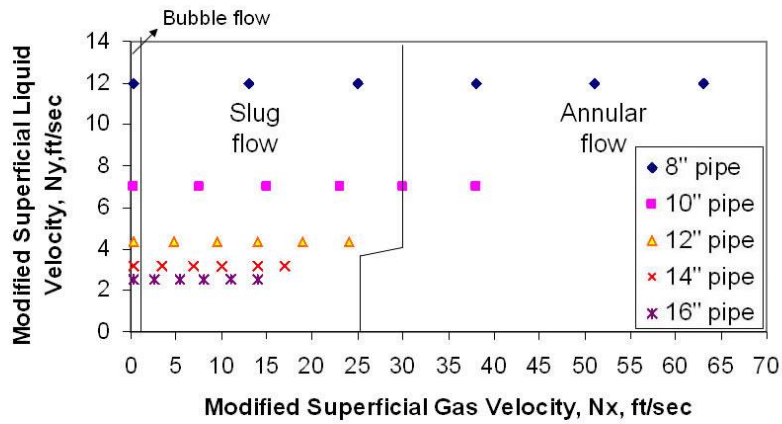

Figure 4.1i: Vertical flow for different internal pipeline diameters at 15,000 bpd

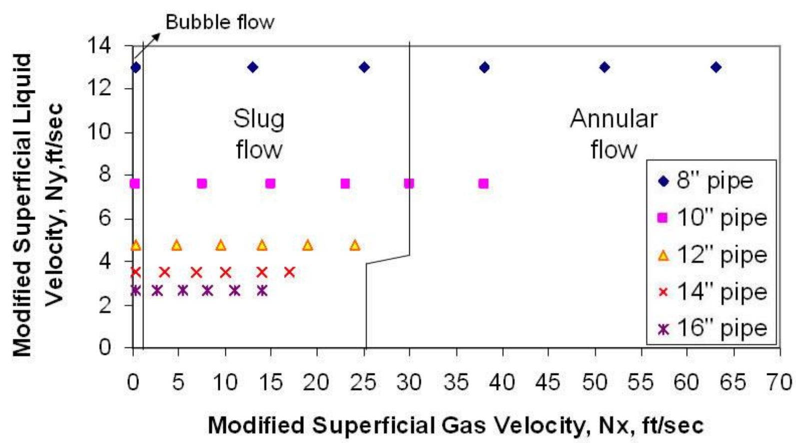

Figure 4.1j: Vertical flow for different internal pipeline diameters at 17,000 bpd

As the trend is observed from Figure 4.1f to Figure 4.1j, 8" – 16" pipeline experiences slug flow at between Nx of 0.1 ft/s to 30 ft/s. However, 12" pipeline experiences froth flow (foam alike) due to its Ny is lower than 3 ft/s and Nx of 25 ft/s at 9,000 bpd and 11,000 bpd as shown in Figure 4.1f and Figure 4.1g.

In addition, 8” to 16” pipeline experiences bubble flow at Nx of 0.1 ft/s regardless any values of Ny. For annular flow, only 8” and 10” pipeline which have more than 30 ft/s of Nx, fall into the annular flow region. It is because when the gas flow rate is increasing, the annular flow begins to dominate the flow from the smallest internal pipeline diameter and so forth. The values in Figure 4.1f to Figure 4.2j which were used to plot those graph can be obtained from Appendix F.

Besides having the calculation and correlation method to determine type of flow for horizontal flow and vertical flow, there are several assumptions and parameters have been made for to ease calculation:

a) The flowline, riser, or pipe is assumed to be a perfect cylinder shape with a cross sectional which any defect-free from buckling or become oval in shape.
b) Due to insufficient data of the fluid flow rate, the oil flow rate is obtained from the expected production flow rate of 120,000 bpd from 9 risers. The average of production flow rate which 13,000 bpd is converted to 0.8 cuft/s as the oil flow rate.
c) In the actual scenario, Kikeh Field is anticipated to produce only oil from the reservoir. However, throughout the time, when the pressure in the reservoir depletes and goes above the bubble point, the gas phase will start to form. Hence, this calculation is also taking gas formation into consideration. The flow rate of gas has been set from 1cuft/s to 5cuft/s with an incremental of 1cuft/s in the type of flow calculations.
d) In addition, 5 different internal pipeline diameters (8”, 10”, 12”, 14, and 16”) have been used to investigate how the flow would be yielded.

4.2 Hydrate Phase Envelope

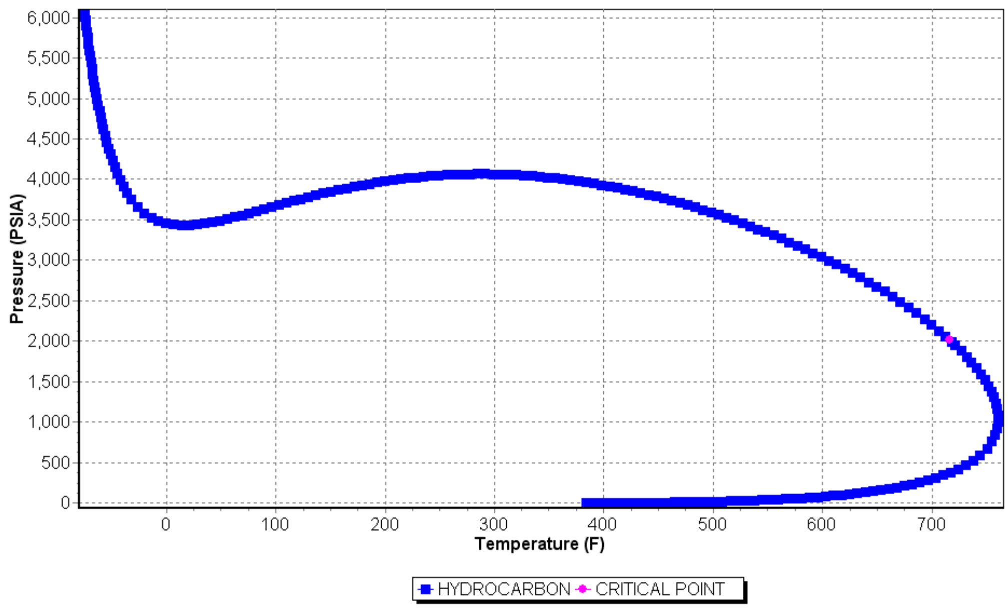

Figure 4.2a: Phase envelope plot with 0% bbl/bbl of water fraction

Figure 4.2a shows that there are no hydrate formation curve and hydrate disassociation curve found at 0% bbl/bbl of water fraction.

The blue color curve represents the hydrocarbon curve with a critical point at about 720 ˚F and 2,000 psia. The curve before the critical point is the bubble point curve and the curve after the critical point is the dew point curve.

The critical point is the point of the transitional point between the dew point curve and bubble point curve.

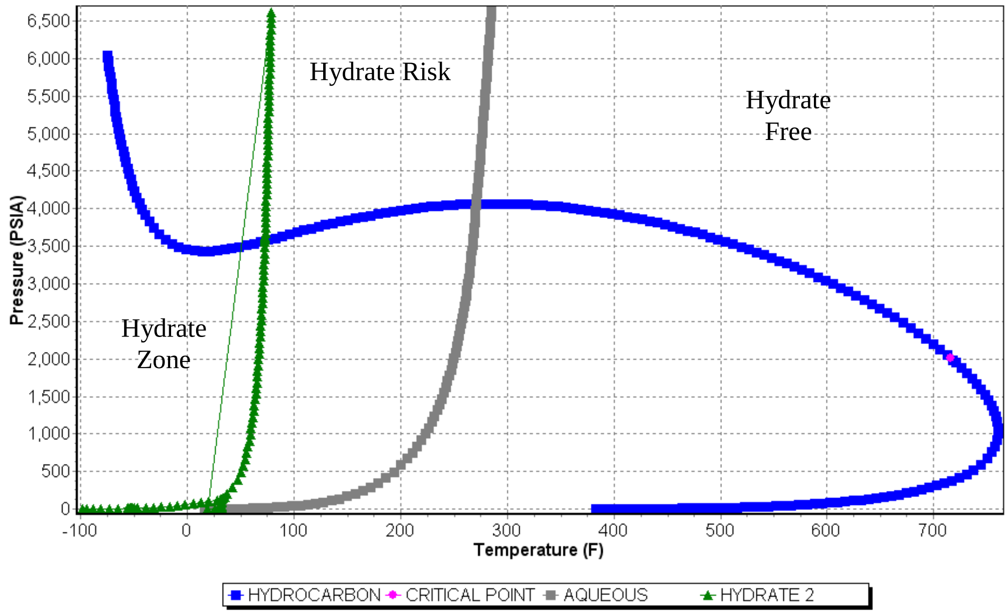

Figure 4.2b: Phase envelope plot with 0.1% bbl/bbl of water fraction

The hydrate formation curve (green curve) and hydrate disassociation curve (grey curve) started to appear when the water fraction is increased to 0.1% bbl/bbl of water fraction in Figure 4.2b.

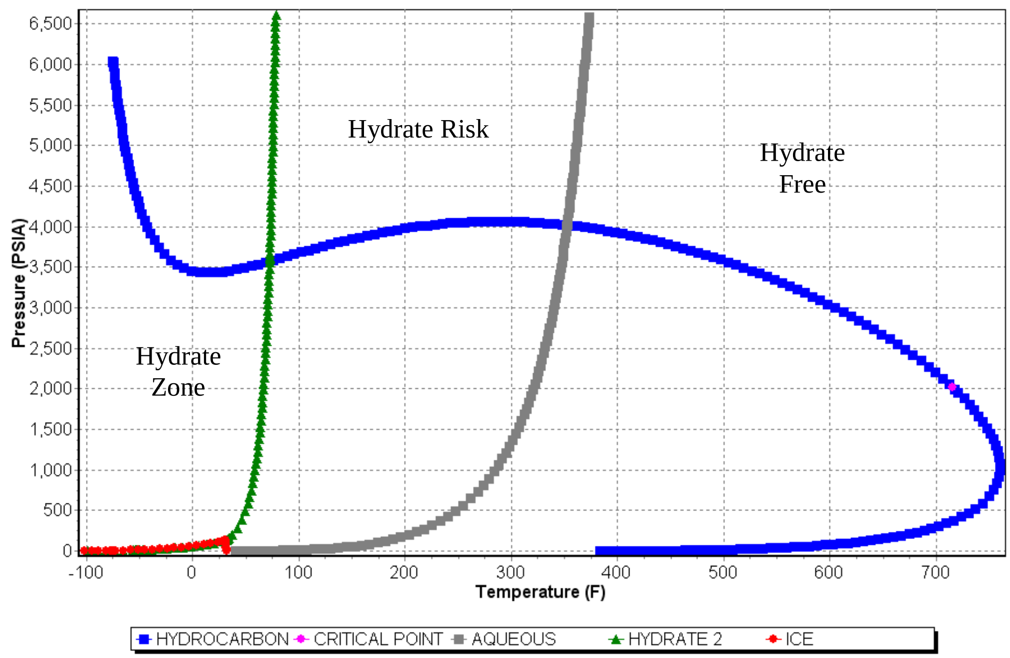

Figure 4.2c: Phase envelope plot with 0.8% bbl/bbl of water fraction

When the water fraction is increased up to 0.8% bbl/bbl (minimum value) of water fraction in Figure 4.2c, the ice formation (red curve) is appeared at about the range of -100 ˚C to 30 ˚C at below 200 psia.

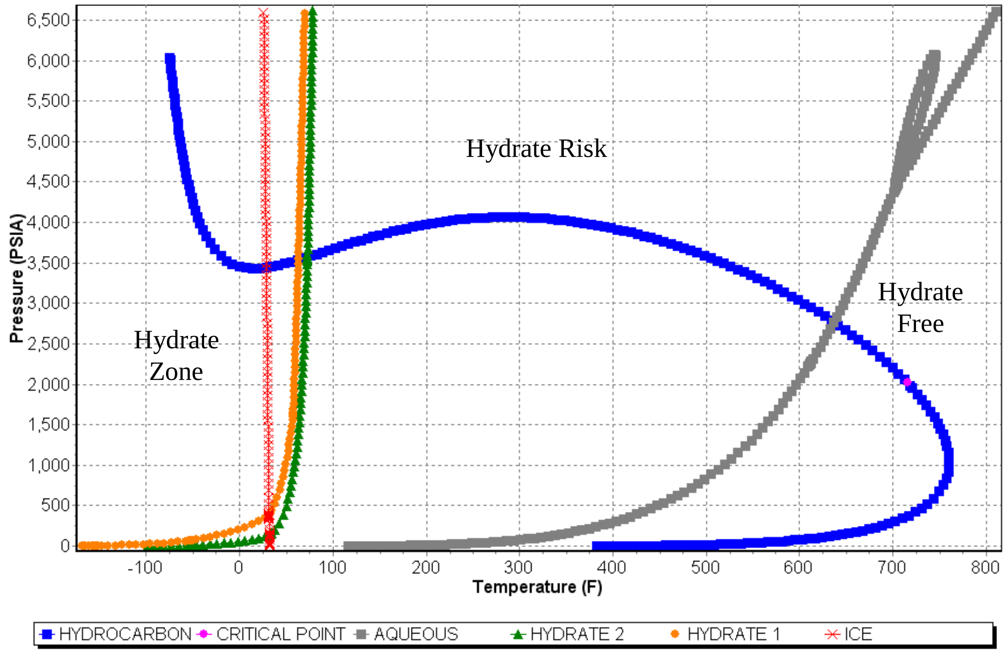

Figure 4.2d: Phase envelope plot with 50% bbl/bbl of water fraction

The water fraction then is further increased up to 50% bbl/bbl of water fraction where the sI hydrate structure (orange curve) is formed. Besides the ice formation (red curve) will occur at about 30 ˚C from 0 psia up to 6500 psia as shown in Figure 4.2d.

At 90% bbl/bbl onwards, there are no results due to the software unable to run the hydrate model as shown in Appendix G.

These simulations show that with present of water in the gas production, the hydrate formation has the tendency to occur at specific temperature and pressure. The preferable temperature for pipeline operating condition is the temperature that is to the right of hydrate disassociation curve (grey curve).

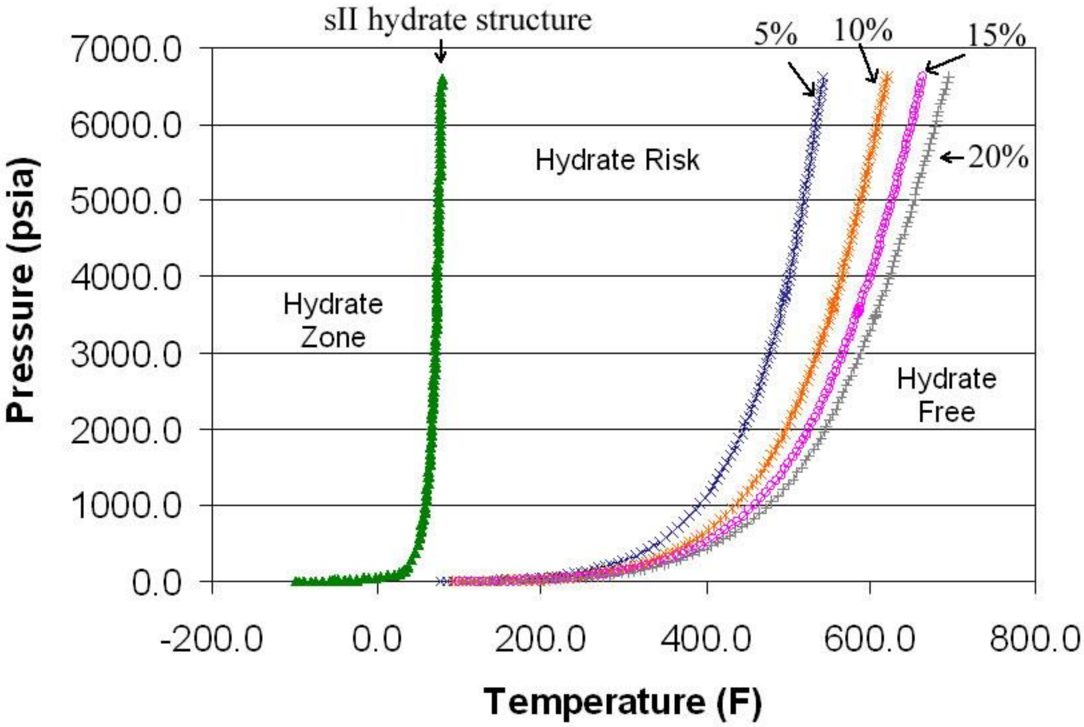

Figure 4.2e: The effect of 'Hydrate Risk' region expansion due to increasing water fraction

Figure 4.2e shows the expansion of hydrate risk region due to the increment of water fraction. However, the hydrate zone region remains the same at every 5% incremental of water fraction.

This proven that higher operating temperature for pipeline is required in order to be in the hydrate free region.

4.3 The Effect of Pressure and Temperature along the Flowline and Riser

4.3.1 The Effect of Temperature along the Flowline and Riser

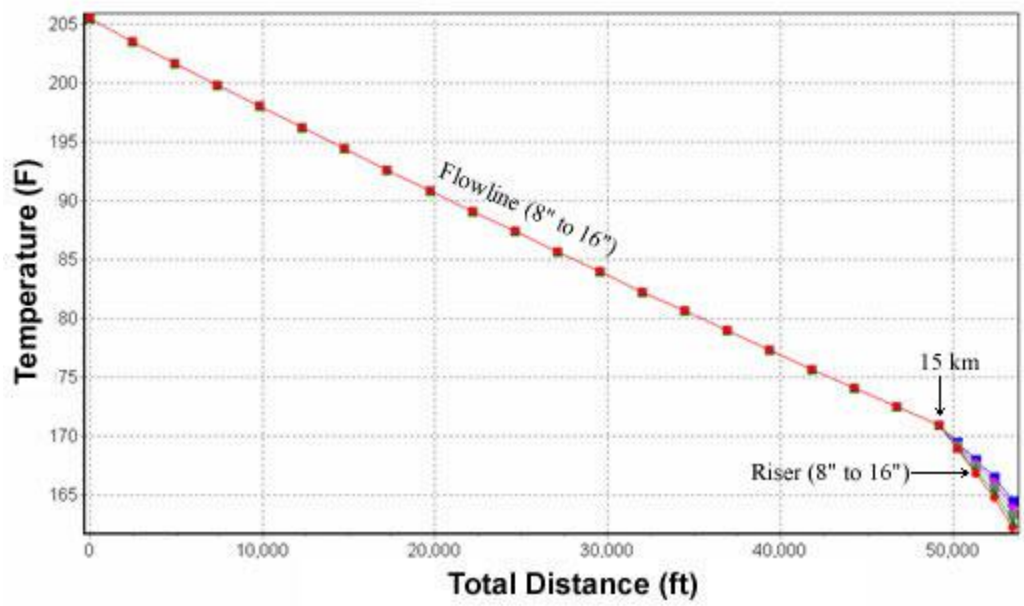

Figure 4.3a: Fluid temperature at different flowline and riser diameters

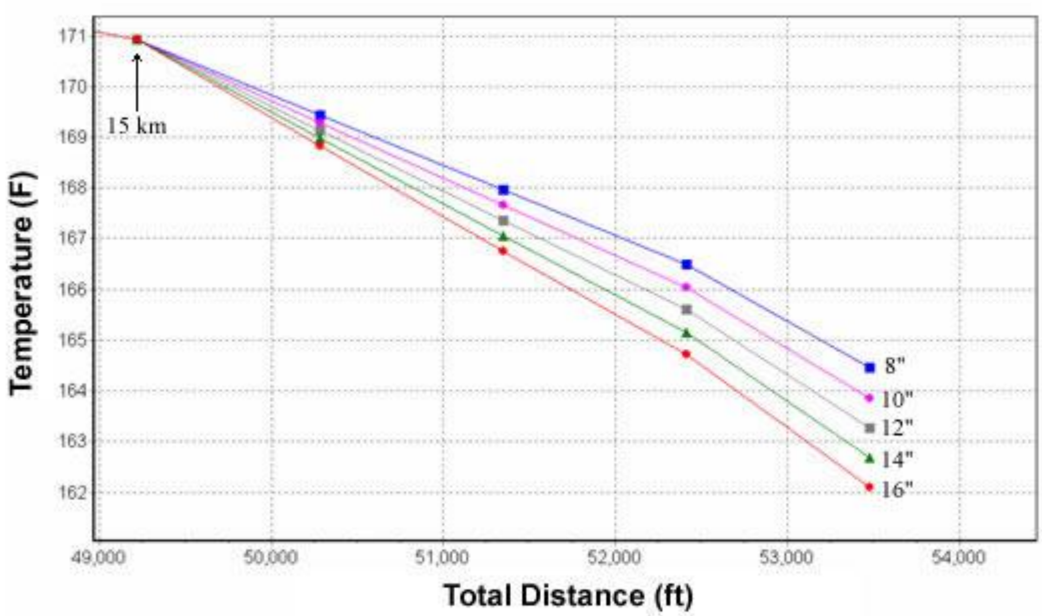

Graph 4.3b: Fluid temperature at different riser diameters

Figure 4.3a shows that the fluid experience heat losses while traveling along the 15 km flowline. At the end of 15 km, the temperature in the riser drop tremendously due to the height of the 1300 m riser. All the data are tabulated in the tables in Appendix H.

The heat losses is due to the abstraction of internal energy (related to the temperatures of the fluids) in to potential energy and to a lesser extent kinetic energy. In addition, some internal energy is employed for the expansion of the fluids up the riser and for latent heat vaporization.

Based on the Figure 4.3b, it shows that the higher the internal pipeline diameter, the lower the temperature it has due larger surface area in the pipeline. Such heat loss serves as one of the criterion in hydrate formation. Therefore, the methods for maintaining the pipeline should be adopted such as pipeline insulation or hot water circulation in the pipeline annulus

4.3.2 The Effect of Pressure along the Flowline and Riser

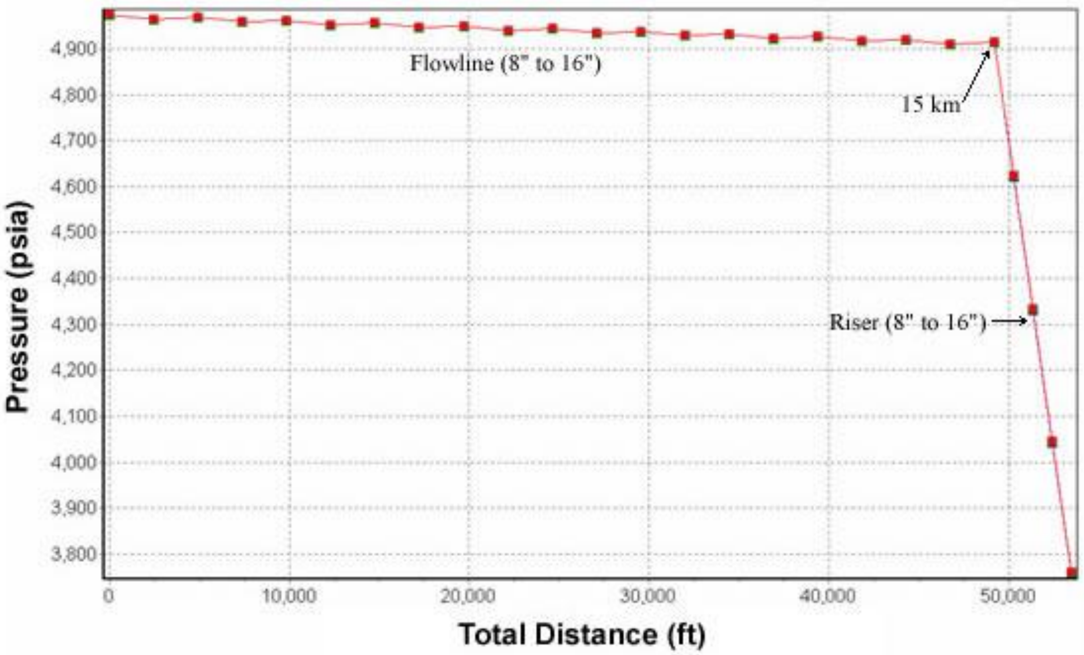

Figure 4.3c: Fluid pressure at different flowline and riser diameter

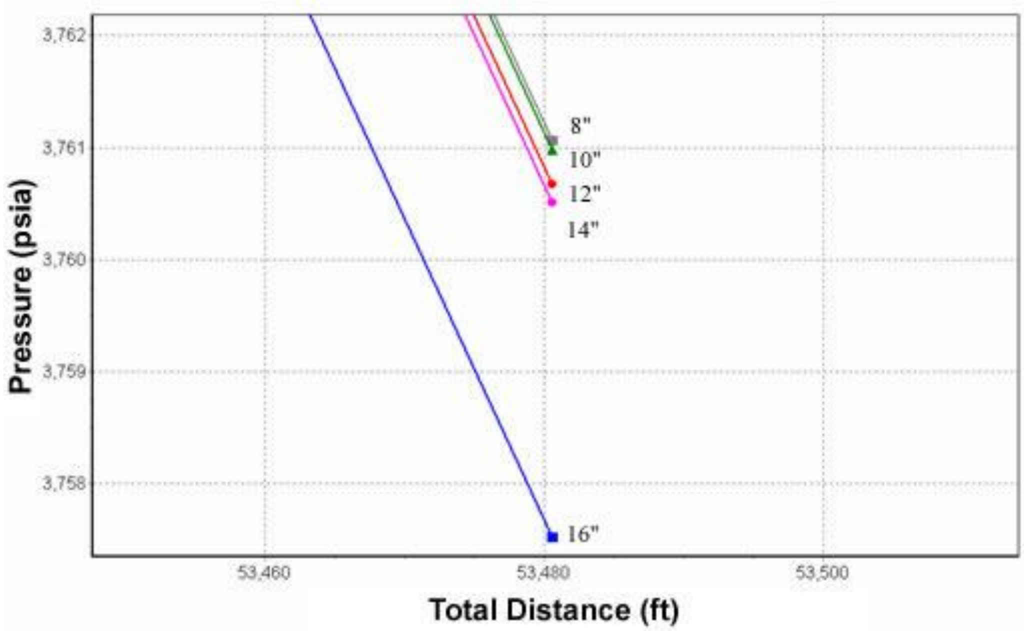

Figure 4.3d: Fluid pressure at different riser diameters

Figure 4.3c shows that the fluid's pressure within the pipeline is almost constant. This is due to the elevation is assumed almost the same along the 15 km flowline

However, the pressure drops signification when the fluid travels upward to the riser top, which due to the decrement of height (from the seabed up to the surface). All the data are tabulated in the tables in Appendix I.

Based on the Figure 4.3d, it shows that the smaller the internal pipeline diameter, the higher the pressure drops. This implies the area is indirectly proportional to the pressure. As shown in Figure 4.2d, besides the guest molecules which are required for hydrate formation, certain temperature and certain pressure have to co-exist together.

CHAPTER 5

CONCLUSION & RECOMMENDATIONS

5.1 Conclusion

Based on the findings, the conclusions of this study are shown as such:

a) Slug flow at horizontal flow

   i) For a fixed gas flow rate at 2 cuft/s, the range for slug flow to occur is at between 8” to 10” of internal pipeline diameter with oil flow rate at 9,000 bpd -15,000 bpd

   ii) The slug flow continue to occur in 8” to 14” of internal pipeline diameter with oil flow rate at 9,000 bpd to 17,000 bpd when the gas flow rate is set to 5 cuft/s.

   iii) This proves that when the gas flow rate is increased, the potential of slug flow to occur is also increased.

   iv) Slug flow tends to occur more in the less internal pipeline diameter at less oil flow rate at a fixed gas flow rate.

b) Slug flow at vertical flow

   i) At 1 cuft/s of gas flow rate, the slug flow occurs at all the internal pipeline diameters of 8” to 16” and oil flow rate range of 9,000 bpd to 15,000 bpd.

   ii) When the gas flow rate is fixed at 3 cuft/s, the annular flow started to replace the slug flow in 8” internal pipeline diameter with the oil flow rate range of 9,000 bpd to 15,000 bpd.

c) Hydrate

   i) When the water fraction is increased from 5% to 20%, the hydrate risk region is expanded to about 30%

   ii) Above 50% bbl/bbl, sII hydrate structure will be formed.

d) Temperature and pressure

   i) As observed, the lowest temperature in the riser is about 160 ˚F and the highest pressure in the riser is about 5,000 psia. By understanding the operating temperature and pressure, this information will be used in the hydrate phase envelope in pipeline design.

5.2 Recommendations

Kikeh Field is expected to achieve the plateau rate of 120,000 bpd in 2009 to 2011. The type of riser used is flexible riser with 12" of internal diameter. Based on this study, there is several range of operating conditions to avoid slug flow which can be applied to the case study as such:

Horizontal flow

a) For a production rate at 9,000 bpd to 13,000 bpd in a single riser, the superficial gas velocity has to be kept below 3 ft/s in order to avoid slug flow.

b) For 15,000 bpd to 17,000 bpd of oil flow rate, the superficial gas velocity has to be maintained below 2.5 ft/s within the bubble flow region.

Vertical flow

a) The slug flow will occur in between 0.1 ft/s and 20 ft/s of modified superficial gas velocity for 9,000 bpd to 11,000 bpd of oil flow rate. Above 20 ft/s, the slug flow will turn into the annular flow. In addition, bubble flow will occur at below 0.1 ft/s of modified superficial gas velocity.

b) For 13,000 bpd, the slug flow is in the range between 0.1ft/s and 25 ft/s of modified superficial gas velocity.

c) For 15,000 bpd and 17,000 bpd, the slug flow is in the range between 0.1 ft/s and 30 ft/s of modified superficial gas velocity.

Hydrate formation

a) The amount of the water content could be varying from time to time which might due to wrong reservoir interpretation or early water influx. Therefore, it is difficult to justify which percentage of water content to be used in the pipeline design.

b) In this study, the lowest temperature in the riser is about 160 ˚F and the highest pressure in the riser is about 5,000 psia. Hence, the designed pipeline should be to withstand 5,000 psia and operates at least about 750 ˚F. Such conditions will prevent the hydrate formation to occur in the pipeline.

Even though the study has provided the operating conditions for the pipeline design, such information are considered to be still insufficient. Hence, further investigations or studies such as cost of fabrication and types of material to be used for riser need to be included in the pipeline design phase. This study provides the preliminary step for the further study of flow characteristic in the deepwater environment.

Due to insufficient time, the author wishes this study can be furthered by carry out the tasks as such:

a) The current study is still consider as primary stage, the severe slugging simulation need to be carried out thru simulation or experiment

b) More studies between different flow correlations have to be carried out to justify the flow patterns.

c) Running simulation/experiment on different shapes of riser, e.g. S-shaped for future implementation

REFERENCES

[1] **P.F. Pickering, G.F. Hewitt, M.J. Watson and C.P. Hale**, The Prediction of Flows in Production Risers - Truth & Myth? FEESA Ltd, 10 Grayswood Drive, Camberley, Surrey, GU16 6AR, 20 October 2003

[2] **Gas Processors Suppliers Association**. 1998. GPSA Engineering Data Book, 11th Edition, Tulsa, OK, USA.

[3] **Hunt**, A. 1996. Fluid properties determine flow line blockage potential, Oil & Gas Journal 94: 62–66.

[4] **Edmonds**, B., Moorwood, R. A. S., and Szczepanski, R. 1998. Hydrate update, GPA Europe Spring Meeting, Darlington, County Durham, UK, May 1998.

[5] **Ali Danesh, "**PVT and Phase Behaviour of Petroleum Reservoir Fluids", Elsevier Science B. V., 2003

[6] **Wilkens,** R. J. 2002. Flow Assurance, In: Fluid Flow Handbook, J. Saleh (Ed.), New York: McGraw-Hill

[7] **Oram**, R. K. 1995. Advances in deepwater pipeline insulation techniques and materials, Deepwater Pipeline Technology Congress, London, UK.

[8] **Mehta**, A. P., Hebert, P. B., and Weatherman, J. P. 2002. Fulfilling the promise of low dosage hydrate inhibitors: journey from academic curiosity to successful field implementations, paper presented at the 2002 Offshore Technology Conference, OTC 14057, Houston, TX, USA.

[9] **Frostman**, L. M. 2000. Anti-aggolomerant hydrate inhibitors for prevention of hydrate plugs in deepwater systems, Proc. SPE Annual Technical Conference and Exhibition, pp. 573–579, Dallas, TX, USA.

[10] **Frostman**, L. M. 2003. Low dosage hydrate inhibitor (LDHI) experience in deepwater, paper presented at the Deep Offshore Technology Conference, Marseille, France.

[11] **Palermo**, T., Argo, C. B., Goodwin, S. P., and Henderson, A. 2000. Flow loop tests on a novel hydrate inhibitor to be deployed in North Sea ETAP field, Annals of the New York Academy of Sciences, New York, 912:355–365

[12] **B.A. Carter**, SPE, Hamersley Iron, and B.F. Ronalds, SPE, "Deepwater Riser Technology", University of Western Australia, SPE 50140

[13] Hewitt, G.F. 1999, Introduction and Basic Models, Chapter 8, pp. 197-203 Handbook of Phase Change, Boiling and Condensation, Editors: S.G. Kandlikar, M. Shoji & V.K. Dhir, Taylor & Francis,Philadelphia

[14] Mandhane, J. M., G. A. Gregory, and K. Aziz. "A Flow Pattern for Map for Gas-Liquid Flow in Horizontal Pipes" Int. J. Multiphase Flow, Pergamon Press, Vol. 1, 1974, pp. 537-553

[15] Aziz, k., G. W. Govier, and M. Fogarasi. "Pressure Drop in wells Producing Oil and Gas" J. Cdn. Pet. Tech., July-Sept 1972, pp.38-48

[16] Schmidt, Z., D.R. Doty, K. Dutta-roy. (1985): severe slugging in offshore pipeline riser-pipe systems. SPE J, pp 27-38.

[17] Zheng, G., J.P. Brill and Y. Taitel (1994): slug flow behaviour in a hilly terrain pipeline. Int. J. Multiphase flow, vol. 20, no 1, pp 63-79

[18] Cem Sarica, SPE, and Jarl Ø. Tengesdal, SPE, The Pennsylvania State University, 2000. A New Technique to Eliminate Severe Slugging in Pipeline/Riser Systems. SPE 63185

APPENDIXES

Appendix A: Gantt Chart

Table 7.1: Final Year Project 1 (Semester 1)

No.	Detail/ Week	1	2	3	4	5	6	7		8	9	10	11	12	13	14
1	Literature Review								Mid-Semester Break							
2	Submission of Preliminary Report															
3	Project Work Continue															
4	Submission of Progress Report 1															
5	Project work continue															
6	Seminar															
7	Submission of Interim Report															
8	Oral Presentation															

Process

Table 7.2: Semester Break

No.	Detail/ Week	1	2	3	4	5	6	7	8
1	Literature Review								
2	Flow Simulation								
3	Data gathering from PETRONAS and TECHNIP								

Process

Table 7.3: Final Year Project 2 (Semester 2)

No.	Detail/ Week	1	2	3	4	5	6	7		8	9	10	11	12	13	14
1	Literature Review	■	■	■	■	■	■	■	Mid-Semester Break	■	■	■	■	■	■	
2	Simulation/ Lab Experiment	■	■	■	■	■	■	■		■	■	■	■	■	■	
3	Meeting with Supervisor	■	■	■	■	■	■	■		■	■	■	■	■	■	■
4	Submission of Progress Report 2				■											
5	Submission of Progress Report 3									■						
6	Submission of Progress Report 4													■		
7	Seminar										■	■	■			
8	Poster Exhibition											■				
9	Submission of Dissertation (soft bound)													■		
10	Oral Presentation and EDX														■	
11	Submission of Project Dissertation (Hard Bound)															■

■ Process

Appendix B: Types of riser

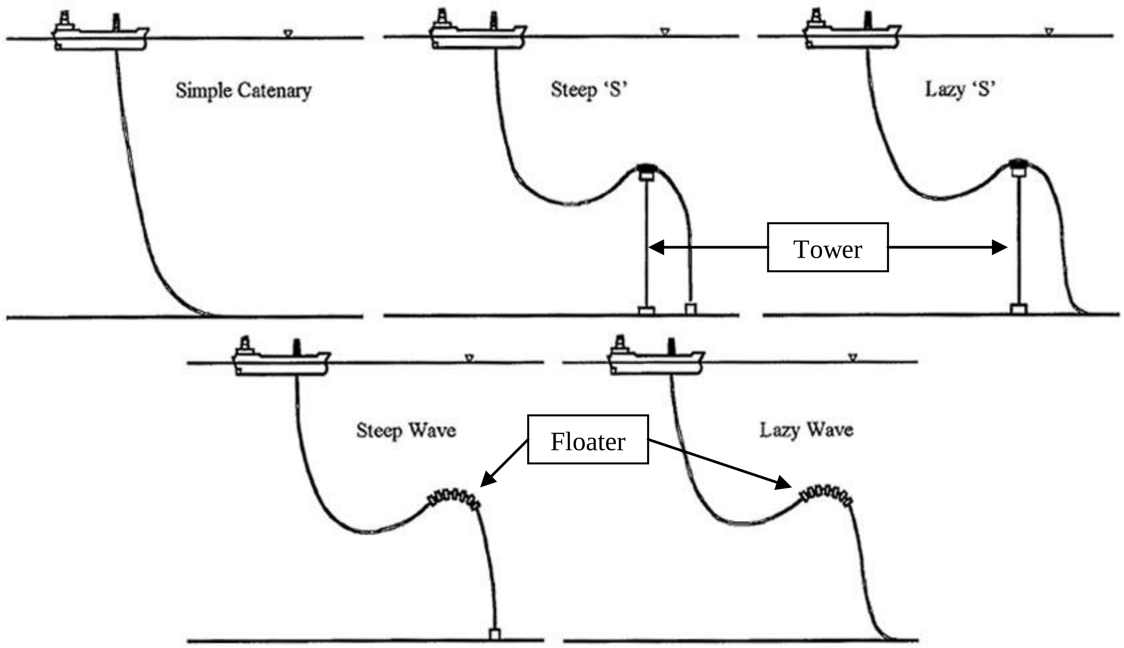

Figure 7.1: Typical flexible riser configurations

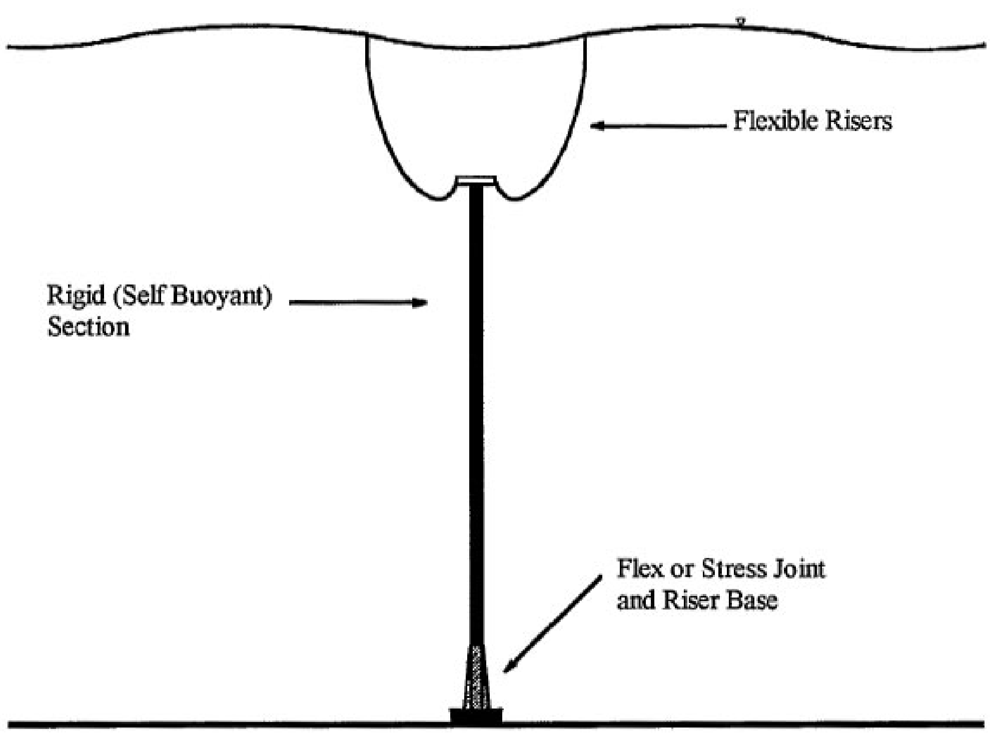

Figure 7.2: Hybrid riser

Appendix C: Flow patterns for horizontal and vertical flows

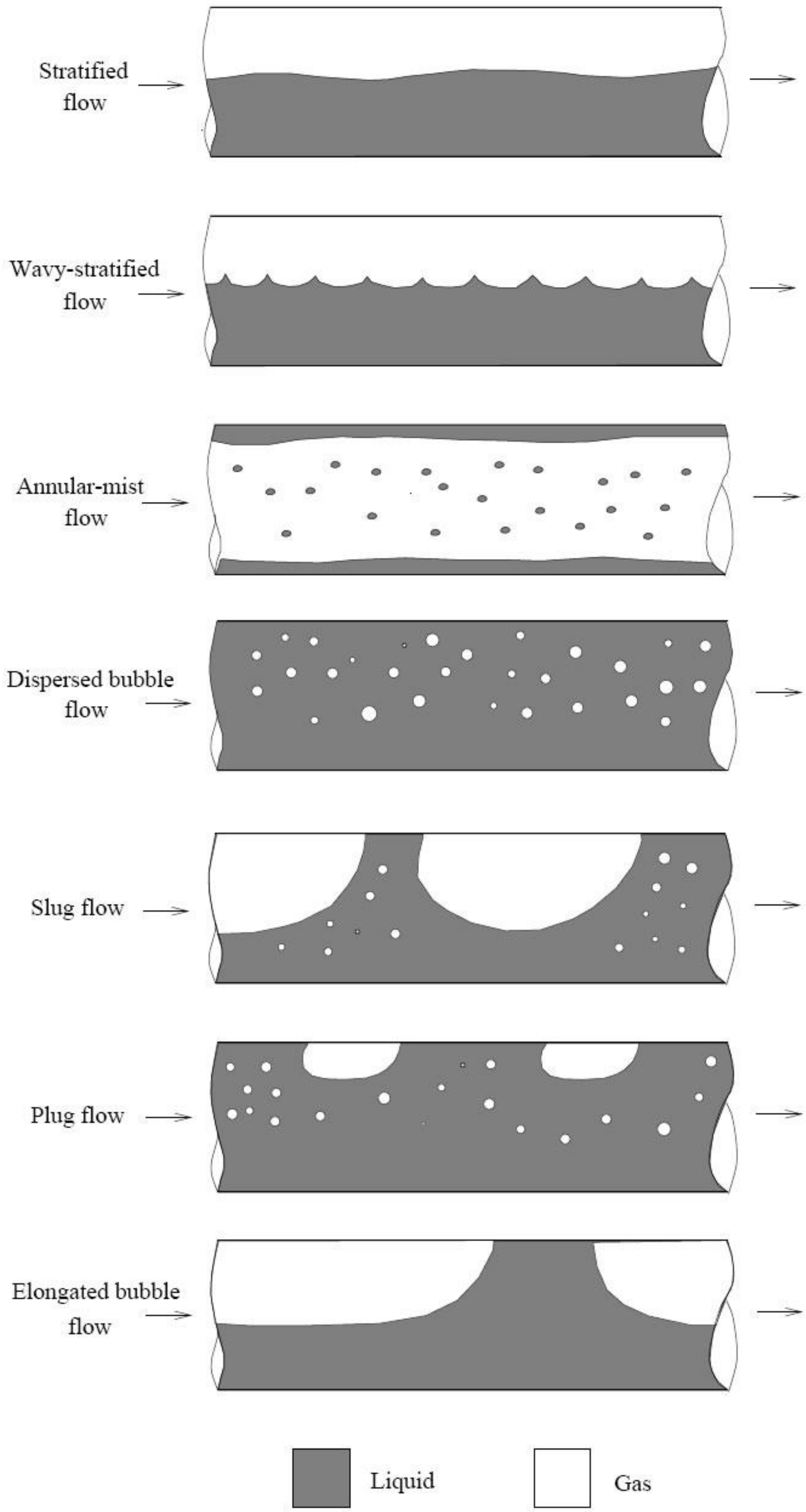

Figure 7.3: Horizontal flow patterns

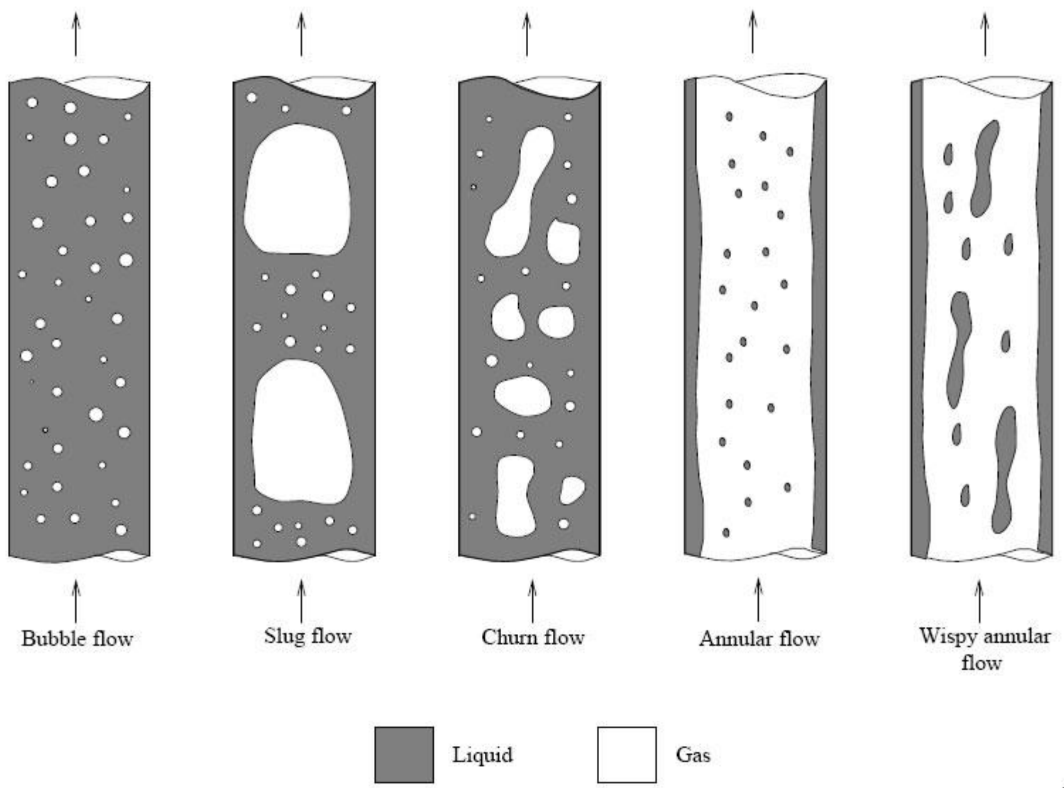

Figure 7.4: Vertical flow patterns

Appendix D: Steps of IFT calculation

a) Calculate the mole component = mole fraction % x molecular weight and find the summation of liquid and gas respectively

b) Based on the chosen pressure at 2000psig, the oil density $\rho_{oil} =$ is 0.806 g/cc. For gas density, given specific gravity is 0.636. By using $S.G. = \frac{\rho_{gas}}{\rho_{air}}$ and the value of ρ_{air} = 0.0009465 g/cc at 205.5 ^{o}F, $\rho_{gas} = 0.000602$ g/cc.

c) Molar density is determined by using $\rho_m = \frac{\rho_i}{M_i}$ for liquid and gas component respectively.

$$\rho_m^{oil} = 4.16x10^{-5}\, gmol/cc$$

$$\rho_m^{gas} = 3.28x10^{-7}\, gmol/cc$$

d) By using the given Parachor values, the IFT is calculated as such

$$\sigma = \sum P_{\sigma i}\left(x_i \rho_m^{oil} - y_i \rho_m^{gas}\right)$$

Table 7.4: Table of IFT value for each hydrocarbon component

Component	MW	Mole % gas	Mole % oil	Mole gas	Mole oil	Parachor	Molar density gas	Molar density oil	IFT
C1	16.0	87.8	0.0	1,408.7	0.0	74.1	0.0	0.0	0.0
C2	30.1	6.7	0.1	200.6	4.2	112.9	0.0	0.0	0.0
C3	44.1	2.5	0.3	109.8	15.0	154.0	0.0	0.0	0.0
i-C4	58.1	0.4	0.1	21.5	8.1	185.3	0.0	0.0	0.0
n-C4	58.1	0.7	0.4	40.7	25.0	193.9	0.0	0.0	0.0
i-C5	72.2	0.2	0.4	15.9	26.7	229.4	0.0	0.0	0.0
n-C5	72.2	0.2	0.5	15.2	33.9	236.0	0.0	0.0	0.0
C6	86.2	0.2	1.4	14.7	120.6	276.7	0.0	0.0	0.0
C7	100.2	0.1	5.0	6.0	500.0	318.4	0.0	0.0	0.1
C8	114.2	0.0	11.2	1.1	1,274.8	359.3	0.0	0.0	0.2
C9	128.3	0.0	7.4	0.0	944.0	399.6	0.0	0.0	0.1
C10	142.3	0.0	5.7	0.0	809.6	440.7	0.0	0.0	0.1
C11	156.3	0.0	4.5	0.0	709.7	482.0	0.0	0.0	0.1
C12	170.3	0.0	7.0	0.0	1,195.8	522.3	0.0	0.0	0.2
C13	184.4	0.0	8.0	0.0	1,474.9	563.8	0.0	0.0	0.2
C14	198.4	0.0	5.9	0.0	1,170.5	606.1	0.0	0.0	0.1
C15	212.4	0.0	5.8	0.0	1,238.4	647.4	0.0	0.0	0.2
C16	226.4	0.0	3.8	0.0	849.2	688.5	0.0	0.0	0.1
C17	240.5	0.0	2.3	0.0	555.5	730.1	0.0	0.0	0.1
C18	254.5	0.0	2.4	0.0	598.1	772.0	0.0	0.0	0.1
C19	268.5	0.0	1.8	0.0	494.1	813.9	0.0	0.0	0.1
C20	282.6	0.0	26.0	0.0	7,337.9	853.7	0.0	0.0	0.9
	TOTAL	98.7	100.0	1,834.1	19,386.0				**2.5**

Appendix E: Steps of horizontal flow and vertical flow calculation

a) Determine the interfacial tension value based on the hydrocarbon component (Appendix D)

b) Determine the superficial liquid velocity, VsL, and the superficial gas velocity, Vsg for horizontal flow

c) Determine the modified superficial liquid velocity, Ny, and the modified superficial gas calculation velocity, Nx for vertical flow calculation

d) The values of VsL and Vsg and the values of Nx and Ny are tabulated in the graph separately according to the production rate.

e) By using Mandhane Horizontal Flow Regime Map, the type of flow is identified based on the value of VsL and Vsg.

f) By using Aziz et al. Vertical Flow Regime Map, the type of flow is identified based on the value of Nx and Ny.

g) The type of flow for horizontal and vertical flow is tabulated in the table

h) Step a – f is repeated with different internal pipeline diameter (8”, 10”, 12”, 14” and 16”) at different gas flow rate (1 cuft/s, 2 cuft/s, 3 cuft/s, 4 cuft/s and 5 cuft/s) and oil flow rate (9,000 bpd, 11,000 bpd, 13,000 bpd, 15,000 bpd, and 17,000 bpd)

i) All types of flow are summarized in the Table 7.5 – 7.29.

Appendix F: Results of horizontal flow and vertical flow calculation

a) Results of horizontal flow and vertical flow at 9,000 bpd of oil

Table 7.5: Result for 8" ID Pipe

Gas flowrate (cuft/s)	Horizontal flow (ft/s)		Vertical Flow (ft/s)	
	VsL	Vsg	Nx	Ny
0.03	2	0.1	0.4	7
1	2	3.3	13	7
2	2	0.7	25	7
3	2	10	38	7
4	2	13.3	51	7
5	2	16.7	63	7

Table 7.6: Result for 10" ID Pipe

Gas flowrate (cuft/s)	Horizontal flow (ft/s)		Vertical Flow (ft/s)	
	VsL	Vsg	Nx	Ny
0.05	1.2	0.1	0.4	4.2
1	1.2	2	7.6	4.2
2	1.2	4	15	4.2
3	1.2	6	23	4.2
4	1.2	8	30	4.2
5	1.2	10	38	4.2

Table 7.7: Result for 12" ID Pipe

Gas flowrate (cuft/s)	Horizontal flow (ft/s)		Vertical Flow (ft/s)	
	VsL	Vsg	Nx	Ny
0.08	0.75	0.1	0.4	2.6
1	0.75	1.3	4.8	2.6
2	0.75	2.5	9.5	2.6
3	0.75	3.8	14	2.6
4	0.75	5	19	2.6
5	0.75	6.3	24	2.6

Table 7.8: Result for 14" ID Pipe

Gas flowrate (cuft/s)	Horizontal flow (ft/s)		Vertical Flow (ft/s)	
	VsL	**Vsg**	**Nx**	**Ny**
0.11	0.5	0.1	0.4	1.9
1	0.5	0.9	3.5	1.9
2	0.5	1.8	6.9	1.9
3	0.5	2.7	10	1.9
4	0.5	3.6	14	1.9
5	0.5	4.5	17	1.9

Table 7.9: Result for 16" ID Pipe

Gas flowrate (cuft/s)	Horizontal flow (ft/s)		Vertical Flow (ft/s)	
	VsL	**Vsg**	**Nx**	**Ny**
0.14	0.4	0.1	0.4	1.5
1	0.4	0.7	2.7	1.5
2	0.4	1.4	5.4	1.5
3	0.4	2.1	8.1	1.5
4	0.4	2.9	11	1.5
5	0.4	3.6	14	1.5

b) Results of horizontal flow and vertical flow at 11,000 bpd of oil

Table 7.10: Result for 8" ID Pipe

Gas flowrate (cuft/s)	Horizontal flow (ft/s)		Vertical Flow (ft/s)	
	VsL	**Vsg**	**Nx**	**Ny**
0.03	2.3	0.1	0.4	8.1
1	2.3	3.3	13	8.1
2	2.3	0.7	25	8.1
3	2.3	10	38	8.1
4	2.3	13.3	51	8.1
5	2.3	16.7	63	8.1

Table 7.11: Result for 10" ID Pipe

Gas flowrate (cuft/s)	Horizontal flow (ft/s)		Vertical Flow (ft/s)	
	VsL	**Vsg**	**Nx**	**Ny**
0.05	1.4	0.1	0.4	4.9
1	1.4	2	7.6	4.9
2	1.4	4	15	4.9
3	1.4	6	23	4.9
4	1.4	8	30	4.9
5	1.4	10	38	4.9

Table 7.12: Result for 12" ID Pipe

Gas flowrate (cuft/s)	Horizontal flow (ft/s)		Vertical Flow (ft/s)	
	VsL	**Vsg**	**Nx**	**Ny**
0.08	0.9	0.1	0.4	3
1	0.9	1.3	4.8	3
2	0.9	2.5	9.5	3
3	0.9	3.8	14	3
4	0.9	5	19	3
5	0.9	6.3	24	3

Table 7.13: Result for 14" ID Pipe

Gas flowrate (cuft/s)	**Horizontal flow (ft/s)**		**Vertical Flow (ft/s)**	
	VsL	**Vsg**	**Nx**	**Ny**
0.11	0.6	0.1	0.4	2.2
1	0.6	0.9	3.5	2.2
2	0.6	1.8	6.9	2.2
3	0.6	2.7	10	2.2
4	0.6	3.6	14	2.2
5	0.6	4.5	17	2.2

Table 7.14: Result for 16" ID Pipe

Gas flowrate (cuft/s)	**Horizontal flow (ft/s)**		**Vertical Flow (ft/s)**	
	VsL	**Vsg**	**Nx**	**Ny**
0.14	0.5	0.1	0.4	1.7
1	0.5	0.7	2.7	1.7
2	0.5	1.4	5.4	1.7
3	0.5	2.1	8.1	1.7
4	0.5	2.9	11	1.7
5	0.5	3.6	14	1.7

c) Results of horizontal flow and vertical flow at 13,000 bpd of oil

Table 7.15: Result for 8" ID Pipe

Gas flowrate (cuft/s)	**Horizontal flow (ft/s)**		**Vertical Flow (ft/s)**	
	VsL	**Vsg**	**Nx**	**Ny**
0.03	2.7	0.1	0.4	9.3
1	2.7	3.3	13	9.3
2	2.7	0.7	25	9.3
3	2.7	10	38	9.3
4	2.7	13.3	51	9.3
5	2.7	16.7	63	9.3

Table 7.16: Result for 10" ID Pipe

Gas flowrate (cuft/s)	**Horizontal flow (ft/s)**		**Vertical Flow (ft/s)**	
	VsL	**Vsg**	**Nx**	**Ny**
0.05	1.6	0.1	0.4	5.6
1	1.4	2	7.6	5.6
2	1.4	4	15	5.6
3	1.4	6	23	5.6
4	1.4	8	30	5.6
5	1.4	10	38	5.6

Table 7.17: Result for 12" ID Pipe

Gas flowrate (cuft/s)	**Horizontal flow (ft/s)**		**Vertical Flow (ft/s)**	
	VsL	**Vsg**	**Nx**	**Ny**
0.08	1	0.1	0.4	3.5
1	1	1.3	4.8	3.5
2	1	2.5	9.5	3.5
3	1	3.8	14	3.5
4	1	5	19	3.5
5	1	6.3	24	3.5

Table 7.18: Result for 14" ID Pipe

Gas flowrate (cuft/s)	Horizontal flow (ft/s)		Vertical Flow (ft/s)	
	VsL	**Vsg**	**Nx**	**Ny**
0.11	0.7	0.1	0.4	2.5
1	0.7	0.9	3.5	2.5
2	0.7	1.8	6.9	2.5
3	0.7	2.7	10	2.5
4	0.7	3.6	14	2.5
5	0.7	4.5	17	2.5

Table 7.19: Result for 16" ID Pipe

Gas flowrate (cuft/s)	Horizontal flow (ft/s)		Vertical Flow (ft/s)	
	VsL	**Vsg**	**Nx**	**Ny**
0.14	0.6	0.1	0.4	2
1	0.6	0.7	2.7	2
2	0.6	1.4	5.4	2
3	0.6	2.1	8.1	2
4	0.6	2.9	11	2
5	0.6	3.6	14	2

d) Results of horizontal flow and vertical flow at 15,000 bpd of oil

Table 7.20: Result for 8" ID Pipe

Gas flowrate (cuft/s)	Horizontal flow (ft/s)		Vertical Flow (ft/s)	
	VsL	**Vsg**	**Nx**	**Ny**
0.03	3.3	0.1	0.4	12
1	3.3	3.3	13	12
2	3.3	0.7	25	12
3	3.3	10	38	12
4	3.3	13.3	51	12
5	3.3	16.7	63	12

Table 7.21: Result for 10" ID Pipe

Gas flowrate (cuft/s)	Horizontal flow (ft/s)		Vertical Flow (ft/s)	
	VsL	**Vsg**	**Nx**	**Ny**
0.05	2	0.1	0.4	7
1	2	2	7.6	7
2	2	4	15	7
3	2	6	23	7
4	2	8	30	7
5	2	10	38	7

Table 7.22: Result for 12" ID Pipe

Gas flowrate (cuft/s)	Horizontal flow (ft/s)		Vertical Flow (ft/s)	
	VsL	**Vsg**	**Nx**	**Ny**
0.08	1.3	0.1	0.4	4.3
1	1.3	1.3	4.8	4.3
2	1.3	2.5	9.5	4.3
3	1.3	3.8	14	4.3
4	1.3	5	19	4.3
5	1.3	6.3	24	4.3

Table 7.23: Result for 14" ID Pipe

Gas flowrate (cuft/s)	**Horizontal flow (ft/s)**		**Vertical Flow (ft/s)**	
	VsL	**Vsg**	**Nx**	**Ny**
0.11	0.9	0.1	0.4	3.2
1	0.9	0.9	3.5	3.2
2	0.9	1.8	6.9	3.2
3	0.9	2.7	10	3.2
4	0.9	3.6	14	3.2
5	0.9	4.5	17	3.2

Table 7.24: Result for 16" ID Pipe

Gas flowrate (cuft/s)	**Horizontal flow (ft/s)**		**Vertical Flow (ft/s)**	
	VsL	**Vsg**	**Nx**	**Ny**
0.14	0.7	0.1	0.4	2.5
1	0.7	0.7	2.7	2.5
2	0.7	1.4	5.4	2.5
3	0.7	2.1	8.1	2.5
4	0.7	2.9	11	2.5
5	0.7	3.6	14	2.5

e) Results of horizontal flow and vertical flow at 17,000 bpd of oil

Table 7.25: Result for 8" ID Pipe

Gas flowrate (cuft/s)	Horizontal flow (ft/s)		Vertical Flow (ft/s)	
	VsL	Vsg	Nx	Ny
0.03	3.7	0.1	0.4	13
1	3.7	3.3	13	13
2	3.7	0.7	25	13
3	3.7	10	38	13
4	3.7	13.3	51	13
5	3.7	16.7	63	13

Table 7.26: Result for 10" ID Pipe

Gas flowrate (cuft/s)	Horizontal flow (ft/s)		Vertical Flow (ft/s)	
	VsL	Vsg	Nx	Ny
0.05	2.2	0.1	0.4	7.6
1	2.2	2	7.6	7.6
2	2.2	4	15	7.6
3	2.2	6	23	7.6
4	2.2	8	30	7.6
5	2.2	10	38	7.6

Table 7.27: Result for 12" ID Pipe

Gas flowrate (cuft/s)	Horizontal flow (ft/s)		Vertical Flow (ft/s)	
	VsL	Vsg	Nx	Ny
0.08	1.4	0.1	0.4	4.8
1	1.4	1.3	4.8	4.8
2	1.4	2.5	9.5	4.8
3	1.4	3.8	14	4.8
4	1.4	5	19	4.8
5	1.4	6.3	24	4.8

Table 7.28: Result for 14" ID Pipe

Gas flowrate (cuft/s)	**Horizontal flow (ft/s)**		**Vertical Flow (ft/s)**	
	VsL	**Vsg**	**Nx**	**Ny**
0.11	1	0.1	0.4	3.5
1	1	0.9	3.5	3.5
2	1	1.8	6.9	3.5
3	1	2.7	10	3.5
4	1	3.6	14	3.5
5	1	4.5	17	3.5

Table 7.29: Result for 16" ID Pipe

Gas flowrate (cuft/s)	**Horizontal flow (ft/s)**		**Vertical Flow (ft/s)**	
	VsL	**Vsg**	**Nx**	**Ny**
0.14	0.8	0.1	0.4	2.7
1	0.8	0.7	2.7	2.7
2	0.8	1.4	5.4	2.7
3	0.8	2.1	8.1	2.7
4	0.8	2.9	11	2.7
5	0.8	3.6	14	2.7

Appendix G: Type of formation at different water fraction in percentage

Table 7.30: Possible formation ice, hydrate I and hydrate II at different water fraction in percentage

Water fraction (%bbl/bbl)	Possible formation (yes/nil)		
	Ice	Hydrate II	Hydrate I
0	Nil	Nil	Nil
0.1	Nil	Yes	Nil
0.8	Yes	Yes	Nil
10	Yes	Yes	Nil
20	Yes	Yes	Nil
30	Yes	Yes	Nil
40	Yes	Yes	Nil
50	Yes	Yes	Yes
60	Yes	Yes	Yes
70	Yes	Yes	Yes
80	Yes	Yes	Yes
90	Nil	Nil	Nil
100	Nil	Nil	Nil

Appendix H: Total distance versus temperature

Table 7.31: Fluid temperature in the different flowline and riser diameter

Total Distance (ft)	Temp. (F)	Total Distance (ft)	Temp. (F)	Total Distance (ft)	Temp. (F)	Total Distance (ft)	Temp. (F)	Total Distance (ft)	Temp. (F)
ID = 8"	ID = 8"	ID = 10"	ID = 10"	ID = 12"	ID = 12"	ID = 14"	ID = 14"	ID = 16"	ID = 16"
0.0	205.5	0.0	205.5	0.0	205.5	0.0	205.5	0.0	205.5
0.0	205.5	0.0	205.5	0.0	205.5	0.0	205.5	0.0	205.5
2,460.8	203.6	2,460.8	203.6	2,460.8	203.6	2,460.8	203.6	2,460.8	203.6
4,921.6	201.7	4,921.6	201.7	4,921.6	201.7	4,921.6	201.7	4,921.6	201.7
7,382.3	199.9	7,382.3	199.9	7,382.3	199.9	7,382.3	199.9	7,382.3	199.9
9,843.1	198.1	9,843.1	198.1	9,843.1	198.1	9,843.1	198.1	9,843.1	198.1
12,303.9	196.2	12,303.9	196.2	12,303.9	196.2	12,303.9	196.2	12,303.9	196.2
14,764.6	194.4	14,764.6	194.4	14,764.6	194.4	14,764.6	194.4	14,764.6	194.4
17,225.4	192.6	17,225.4	192.6	17,225.4	192.6	17,225.4	192.6	17,225.4	192.6
19,686.2	190.9	19,686.2	190.9	19,686.2	190.9	19,686.2	190.9	19,686.2	190.9
22,147.0	189.1	22,147.0	189.1	22,147.0	189.1	22,147.0	189.1	22,147.0	189.1
24,607.7	187.4	24,607.7	187.4	24,607.7	187.4	24,607.7	187.4	24,607.7	187.4
27,068.6	185.6	27,068.6	185.6	27,068.6	185.6	27,068.6	185.6	27,068.6	185.6
29,529.3	184.0	29,529.3	184.0	29,529.3	184.0	29,529.3	184.0	29,529.3	184.0
31,990.1	182.3	31,990.1	182.3	31,990.1	182.3	31,990.1	182.3	31,990.1	182.3
34,450.8	180.6	34,450.8	180.6	34,450.8	180.6	34,450.8	180.6	34,450.8	180.6
36,911.6	178.9	36,911.6	178.9	36,911.6	178.9	36,911.6	178.9	36,911.6	178.9
39,372.4	177.3	39,372.4	177.3	39,372.4	177.3	39,372.4	177.3	39,372.4	177.3
41,833.2	175.7	41,833.2	175.7	41,833.2	175.7	41,833.2	175.7	41,833.2	175.7
44,293.9	174.1	44,293.9	174.1	44,293.9	174.1	44,293.9	174.1	44,293.9	174.1
46,754.6	172.5	46,754.6	172.5	46,754.6	172.5	46,754.6	172.5	46,754.6	172.5
49,215.5	170.9	49,215.5	170.9	49,215.5	170.9	49,215.5	170.9	49,215.5	170.9
50,281.7	169.4	49,215.5	170.9	49,215.5	170.9	49,215.5	170.9	49,215.5	170.9
51,348.0	168.0	50,281.7	169.3	50,281.7	169.1	50,281.7	169.0	50,281.7	168.8
52,414.3	166.5	51,348.0	167.7	51,348.0	167.4	51,348.0	167.1	51,348.0	166.8
53,480.6	164.4	52,414.3	166.0	52,414.3	165.6	52,414.3	165.2	52,414.3	164.7
53,480.6	164.4	53,480.6	163.9	53,480.6	163.3	53,480.6	162.7	53,480.6	162.1

Appendix I: Total distance versus pressure

Table 7.32: Fluid pressure in the different flowline and riser diameter

Total Distance (ft)	Pressure (psia)	Total Distance (ft)	Pressure (psia)	Total Distance (ft)	Pressure (psia)	Total Distance (ft)	Pressure (psia)	Total Distance (ft)	Pressure (psia)
ID = 8"	ID = 8"	ID = 10"	ID = 10"	ID = 12"	ID = 12"	ID = 14"	ID = 14"	ID = 16"	ID = 16"
0.0	4,973.7	0.0	4,973.7	0.0	4,973.7	0.0	4,973.7	0.0	4,973.7
0.0	4,973.7	0.0	4,973.7	0.0	4,973.7	0.0	4,973.7	0.0	4,973.7
2,460.8	4,964.2	2,460.8	4,964.2	2,460.8	4,964.2	2,460.8	4,964.2	2,460.8	4,964.2
4,921.6	4,967.8	4,921.6	4,967.8	4,921.6	4,967.8	4,921.6	4,967.8	4,921.6	4,967.8
7,382.3	4,958.2	7,382.3	4,958.2	7,382.3	4,958.2	7,382.3	4,958.2	7,382.3	4,958.2
9,843.1	4,961.8	9,843.1	4,961.8	9,843.1	4,961.8	9,843.1	4,961.8	9,843.1	4,961.8
12,303.9	4,952.2	12,303.9	4,952.2	12,303.9	4,952.2	12,303.9	4,952.2	12,303.9	4,952.2
14,764.6	4,955.8	14,764.6	4,955.8	14,764.6	4,955.8	14,764.6	4,955.8	14,764.6	4,955.8
17,225.4	4,946.2	17,225.4	4,946.2	17,225.4	4,946.2	17,225.4	4,946.2	17,225.4	4,946.2
19,686.2	4,949.8	19,686.2	4,949.8	19,686.2	4,949.8	19,686.2	4,949.8	19,686.2	4,949.8
22,147.0	4,940.2	22,147.0	4,940.2	22,147.0	4,940.2	22,147.0	4,940.2	22,147.0	4,940.2
24,607.7	4,943.9	24,607.7	4,943.9	24,607.7	4,943.9	24,607.7	4,943.9	24,607.7	4,943.9
27,068.6	4,934.2	27,068.6	4,934.2	27,068.6	4,934.2	27,068.6	4,934.2	27,068.6	4,934.2
29,529.3	4,937.9	29,529.3	4,937.9	29,529.3	4,937.9	29,529.3	4,937.9	29,529.3	4,937.9
31,990.1	4,928.3	31,990.1	4,928.3	31,990.1	4,928.3	31,990.1	4,928.3	31,990.1	4,928.3
34,450.8	4,932.0	34,450.8	4,932.0	34,450.8	4,932.0	34,450.8	4,932.0	34,450.8	4,932.0
36,911.6	4,922.3	36,911.6	4,922.3	36,911.6	4,922.3	36,911.6	4,922.3	36,911.6	4,922.3
39,372.4	4,926.0	39,372.4	4,926.0	39,372.4	4,926.0	39,372.4	4,926.0	39,372.4	4,926.0
41,833.2	4,916.3	41,833.2	4,916.3	41,833.2	4,916.3	41,833.2	4,916.3	41,833.2	4,916.3
44,293.9	4,920.1	44,293.9	4,920.1	44,293.9	4,920.1	44,293.9	4,920.1	44,293.9	4,920.1
46,754.6	4,910.4	46,754.6	4,910.4	46,754.6	4,910.4	46,754.6	4,910.4	46,754.6	4,910.4
49,215.5	4,914.1	49,215.5	4,914.1	49,215.5	4,914.1	49,215.5	4,914.1	49,215.5	4,914.1
50,281.7	4,622.5	49,215.5	4,914.1	49,215.5	4,914.1	49,215.5	4,914.1	49,215.5	4,914.1
51,348.0	4,332.2	50,281.7	4,623.3	50,281.7	4,623.5	50,281.7	4,623.6	50,281.7	4,623.6
52,414.3	4,043.2	51,348.0	4,333.8	51,348.0	4,334.3	51,348.0	4,334.4	51,348.0	4,334.4
53,480.6	3,757.5	52,414.3	4,045.6	52,414.3	4,046.2	52,414.3	4,046.4	52,414.3	4,046.3
53,480.6	3,757.5	53,480.6	3,760.5	53,480.6	3,761.1	53,480.6	3,761.0	53,480.6	3,760.7